Fragment-based drug design targeting syntenin PDZ2 domain involved in exosomal release and tumour spread

Manon Garcia, Laurent Hoffer, Raphaël Leblanc, Fatiha Benmansour, Mikael Feracci, Carine Derviaux, Antonio Luis Egea-Jimenez, Philippe Roche, Pascale Zimmermann, Xavier Morelli, et al.

Fragment-based drug design targeting syntenin PDZ2 domain involved in exosomal release and tumour spread

Manon Garcia[a], Laurent Hoffer[a], Raphaël Leblanc[b], Fatiha Benmansour[a], Mikael Feracci[a], Carine Derviaux[a], Antonio Luis Egea-Jimenez[b], Philippe Roche[a], Pascale Zimmermann[b,c], Xavier Morelli[a] and Karine Barral[a,*]

[a]Centre de Recherche en Cancérologie de Marseille (CRCM), Integrative Structural & Chemical Biology, Aix-Marseille Université, Inserm 1068, CNRS 7258, Institut Paoli Calmettes, 13009 Marseille, France

[b]Equipe labellisée Ligue 2018, Centre de Recherche en Cancérologie de Marseille, Aix-Marseille Université, Inserm1068, CNRS7258, Institut Paoli-Calmettes, 13009 Marseille, France

[c]Department of Human Genetics, K. U. Leuven, B-3000 Leuven, Belgium

[*]Correspondence should be addressed to Karine Barral

Email adress: karine.barral@inserm.fr

Abbreviations: FBDD, fragment-based drug design; PPI, protein-protein interaction; PDB, protein data bank; LE, ligand efficiency; LLE, lipophilic Ligand Efficiency; BB, building block; IC_{50}, inhibitory concentration needed to decrease by 50% the enzyme activity; EC_{50}, effective concentration inducing 50% of the maximum effect on infected cells; CC_{50}, cytotoxic

concentration that reduces the infected cell number by 50% ; SD, standard deviation; HTRF, Homogeneous Time Resolved Fluorescence; LC/MS, liquid chromatography / mass spectroscopy; NMR, nuclear magnetic resonance; rt, room temperature; EDCI, 1-ethyl-3-(3-dimethylaminopropyl)carbodiimide; THF, tetrahydrofuran; FA, formic acid; VS, virtual screening; SAR, Structure-activity relationship.

Abstract

Syntenin stimulates exosome production and its expression is upregulated in many cancers and implicated in the spread of metastatic tumor. These effects are supported by syntenin PDZ domains interacting with syndecans. We therefore aimed to develop, through a fragment-based drug design approach, novel inhibitors targeting syntenin-syndecan interactions. We describe here the optimization of a fragment, 'hit' **C58**, identified by *in vitro* screening of a PDZ-focused fragment library, which binds specifically to the syntenin-PDZ2 domain at the same binding site as the syndecan-2 peptide. X-ray crystallographic structures and computational docking were used to guide our optimization process and lead to compounds **45** and **57** (IC_{50} = 33 µM and 47 µM; respectively), two representatives of syntenin-syndecan interactions inhibitors, that selectively affect the syntenin-exosome release. These findings demonstrate that it is possible to identify small molecules inhibiting syntenin-syndecan interaction and exosome release that may be useful for cancer therapy.

Keywords:

Fragment-based drug design

Small molecule PPI inhibitor

Syntenin-Syndecan interaction inhibitors

Exosomes biogenesis

Cancer therapy

1- Introduction

Exosomes are lipid-bilayer nanovesicles, released from most cell types, which appear to be important during cancer progression, with a role in metastatic niche formation and tumor immune escape [1, 2]. 'Cancer exosomes' derived from tumor cells are thus gaining considerable attention as oncotargets [3]. Syntenin, a 32 kDa PDZ-tandem (PDZ1 and PDZ2) intracellular protein, has a large variety and diversity of interaction partners, including syndecans [4]. Syndecans (SDCs) are transmembrane proteins carrying heparin sulfate chains involved in numerous cellular processes, including cell–cell and cell–matrix adhesion, signal transduction, and vesicular trafficking [5-7]. P. Zimmermann and coworkers have identified a molecular pathway, supported by the syndecan heparan sulfate proteoglycans and their adaptor protein syntenin, that binds to the cytosolic tail of syndecans, which regulates the biogenesis and the uptake of a specific subclass of exosome [8]. Recent studies established that syntenin-exosomes might be implicated in the processes of malignant cell invasion and the establishment of niches that promote tumor metastasis [9]. Indeed, syntenin expression is upregulated in many cancer cell lines (carcinomas and others cancers) suggesting that it may be an effective target to intervene in metastasis since gain of syntenin expression in tumors cells has been associated with the invasion and the metastatic potential of various solid cancers [10].

As knowledge has grown regarding cellular protein interaction networks and their role in numerous cell disorders, including cancer, targeting protein-protein interactions (PPI) has emerged as an encouraging therapeutic approach for the treatment of solid tumors or hematologic malignancies [11-13]. Promising results have been obtained with PPI inhibitors such as p53, BclxL or more recently bromodomain inhibitors [13-18]. We therefore aim to apply a Fragment-Based Drug Design (FBDD) strategy for the rapid identification of starting

hits and their subsequent optimization into compounds that can selectively disrupt syntenin-syndecan PDZ-domain mediated interactions showing known implications in cancer development and dissemination.

In a previous study, Leblanc *et al.* screened a fragment library, containing 139 potential PDZ-inhibitory fragments, on syntenin-syndecan-2 complex by HTRF. Five fragments were identified and tested for their selectivity in two other PDZ-mediated interaction complexes implicated in oncology, namely GRASP/Jam-C and Erbin/P0071 complexes [19]. The most potent and selective fragment, **C58** (Figure 1), was confirmed in a secondary dose-response screening to be a reliable inhibitor of syntenin-syndecan interaction with an IC_{50} of 350 µM (LE = 0.25). Additional experiment on MCF7 breast carcinoma cells established that **C58** decreases MCF7 migration and colony formation, alters mammosphere formation and exosomal release [19]. Taken together, these data clearly indicated that fragment **C58** is a selective inhibitor of the syntenin-exosomal pathway.

It should be noted that PDZ domains belong to protein-protein interaction (PPI) networks, and were considered as poorly druggable targets for the development of potent small organic probes. This was confirmed by the screening of large compound libraries in which no potent hits were identified [20]. However, several studies have reported that small organic compounds were able to disrupt PPIs between PDZ domains and their endogenous protein partners [21]. Some of these studies also included intensive structure–activity relationship (SAR) studies in which dozens analogs were synthesized and tested. As expected, due to the poor druggable nature of PDZ domains, most non-peptide compounds exhibited moderate inhibition, *i.e.* IC_{50} in the 10 micromolar range. One notable exception was recently reported with the development of high affinity compounds (IC_{50} value below 100 nM) for the Pick1 PDZ domain [22]. To our knowledge, this is the most potent non-peptide PDZ inhibitor discovered to date. Regarding the

syntenin protein, the most potent organic compound reported to date targeted its first PDZ domain and had a K_d value of 21 µM (LE = 0.16) [23]. In this study, we performed SAR analysis and fragment hit optimization aiming to improve the affinity of **C58** for the second PDZ domain of Syntenin. X-ray crystallographic structures and molecular modeling were used to guide the fragment optimization process in order to generate new analogues by adding chemical groups that might establish strong interactions with syntenin-PDZ2 domain.

2- Results and discussion

*2-1. Fragment expansion and SAR around analogues of **C58***

A hit identified from screening traditionally require expansion to provide evidence SAR based upon chemical similarity. Therefore, fragment **C58** was used as starting point to select the best fragment hit involved in the subsequent optimization process. For this purpose, a rapid fragment hit expansion has been considered by synthetizing nearest analogues around fragment **C58** (Figure 1).

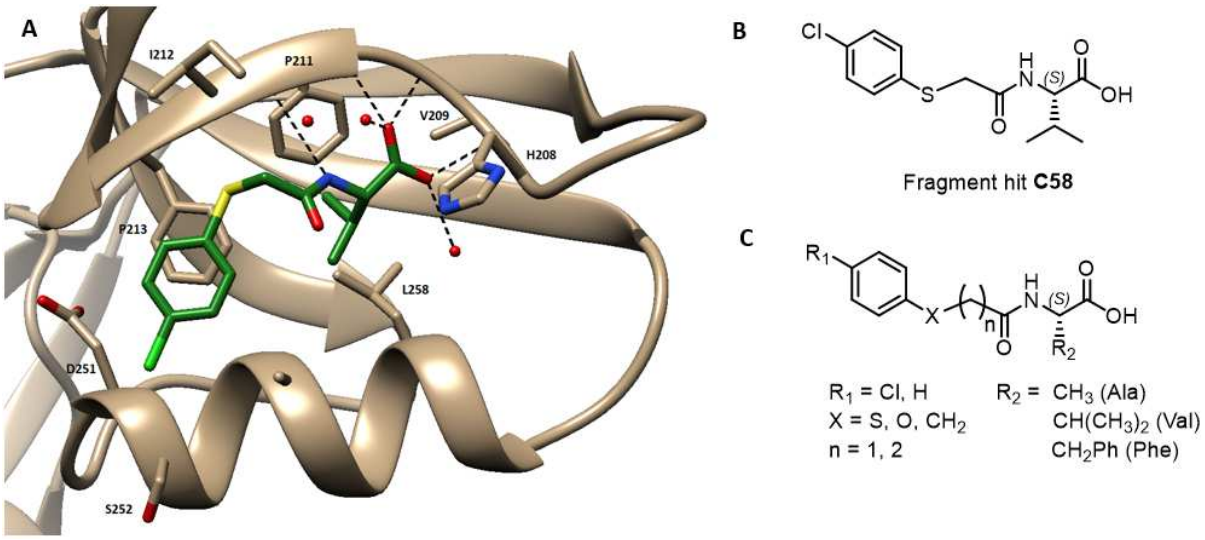

Figure 1. A. Crystal structure of syntenin PDZ2 domain in complex with compound **C58** (PDBID: 6R9H). Compound **C58** is depicted in cylinder representation dark green carbon atom. Nitrogen, oxygen, chlorine and sulfur are colored in blue, red, green and yellow, respectively. Small red spheres represent water molecules around the binding sites. Hydrogen bond interactions are displayed as black dotted lines. Amino acid residues highlighted are those establishing Van der Waals interactions with compound **C58**. **B**. 2D structure of hit fragment **C58**. **C**. 2D structures of putatively interesting explored modifications around fragment **C58**.

X-ray crystal structure of **C58** bound to syntenin was resolved (PDB code 6R9H) and revealed that **C58** is located within the syntenin-PDZ2 domain on the same binding pocket as syndecan-2 peptide as shown in Figure 1A (a superimposition view of binding mode of compounds **C58** and C-terminal end peptide of Syndecan is given Figure S1A in Supp. Data). The phenyl ring of fragment **C58** exhibits a strong π-stacking with Phe213, its nitrogen atom interacts with the backbone carbonyl of Phe211 through hydrogen bonds and its carboxylic acid forms the expected canonical hydrogen-bonding interactions with backbone amide group of Val209 and Gly210 [19]. Based on these structural data, we explored four different modifications to improve the affinity of **C58** while maintaining its canonical binding mode (Figure 1C).

The main modification involved the terminal hydrophobic moiety of fragment **C58**. Indeed, PDZ domains are known to recognize C-terminal hydrophobic moieties from their partners. The last residue from syntenin endogenous ligands (syndecan proteins) is an alanine that contains a very small hydrophobic sidechain. Surprisingly, structural data highlighted that PDZ domain from syntenin was also able to bind peptides with large hydrophobic terminal residue (PDB 1W9E). However, binding of the phenylalanine required an induced fit to accommodate the large benzyl group. Thus, 3 different terminal modifications (Ala-like, Val-like and Phe-like) were investigated in the SAR studies. A thioether function was also present in the original

fragment hit. This sub-optimal moiety, from a medicinal chemistry point of view, was replaced by 1) its similar ether function and 2) with one methylene spacer in the SAR studies. Finally, the influence of the chlorine atom was also assessed by synthesizing the chlorine-free version of each compound.

In a first stage, we aimed to synthesize analogues with a spacer length of two atoms (S-CH_2 or O-CH_2) between the phenyl ring and the amide bond. A general synthesis of amide derivatives is depicted in Scheme 1. To proceed, we directly condensed the commercial acetyl chloride derivatives (**1-4**) with the corresponding L-aminoacid methyl ester hydrochloride (Alanine or Valine) in a mixture dichloromethane/trimethylamine at room temperature [24]. Methyl ester intermediates **5-12** obtained with good to excellent yields were then hydrolysed with LiOH to give derivatives **13-20** [25].

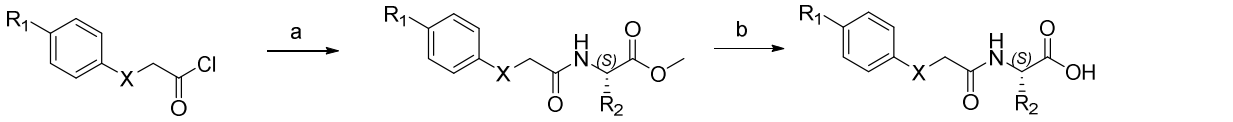

1-2 X = S, R_1 = H, Cl
3-4 X = O, R_1 = H, Cl

Compounds	X	R_1	R_2
5	S	H	CH_3
6			$CH(CH_3)_2$
7	S	Cl	CH_3
8			$CH(CH_3)_2$
9	O	H	CH_3
10			$CH(CH_3)_2$
11	O	Cl	CH_3
12			$CH(CH_3)_2$

Compounds	X	R_1	R_2
13	S	H	CH_3
14			$CH(CH_3)_2$
15	S	Cl	CH_3
16 (C58)			$CH(CH_3)_2$
17	O	H	CH_3
18			$CH(CH_3)_2$
19	O	Cl	CH_3
20			$CH(CH_3)_2$

Reagents and conditions: (a) L-aminoacid methyl ester hydrochloride, Et_3N, dry CH_2Cl_2, 4°C-rt, 2-4h; (b) LiOH, THF/H_2O, 0°C-rt, 1h.

Scheme 1. Synthesis of analogues **13-20**.

In a second stage, we performed the synthesis of analogues with a spacer length of three atoms (S-CH_2-CH_2, O-CH_2-CH_2 or $(CH_2)_3$) between the phenyl ring and the amide bond (Scheme 2). Indeed, molecular modeling studies, relying on the X-ray structure of **C58 (16)**, suggested that the addition of one carbon spacer in the compound structure could maintain both the PDZ

canonical binding mode with the carboxylate group and π-stacking with Phe213, while optimizing the torsion angles from the flexible carbohydrate spacer.

Thus, thiophenol and 4-chlorothiophenol were converted to 3-(phenylthio)propanoic acid **23** and 3-(4-chlorophenylthio)propanoic acid **24** by S-alkylation with 3-chloropropionic acid under alkaline conditions [26, 27]. Then, derivatives **23** and **24**, as well as commercial propionic acid derivatives **25-27**, were condensed with the corresponding L-aminoacid methyl ester hydrochloride (Alanine, Valine or Phenylalanine) in a mixture dichloromethane/trimethylamine at room temperature in the presence of coupling reagent EDCI [28, 29]. As previously, methyl ester intermediates **28-40** obtained with good yields were then hydrolysed with LiOH to give derivatives **41-53** [25].

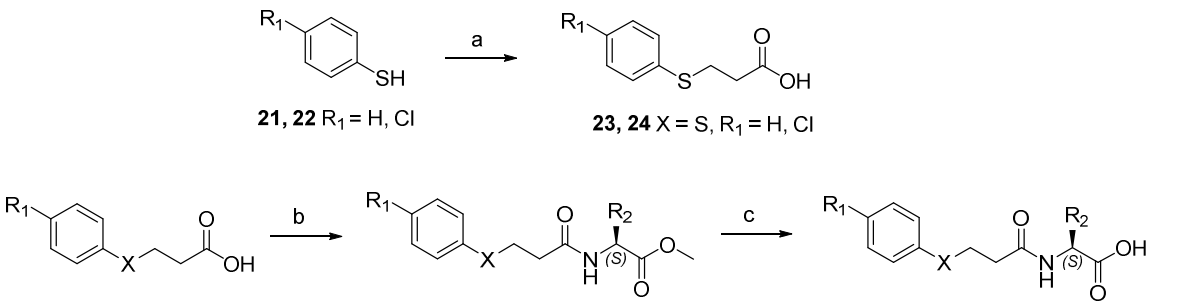

23, 24 X = S, R_1 = H,Cl
25, 26 X = O, R_1 = H, Cl
27 X = CH_2, R_1 = H

Compounds	X	R_1	R_2
28	S	H	CH_3
29			$CH(CH_3)_2$
30			CH_2Ph
31	S	Cl	CH_3
32			$CH(CH_3)_2$
33			CH_2Ph
34	O	H	CH_3
35			$CH(CH_3)_2$
36			CH_2Ph
37	O	Cl	CH_3
38			$CH(CH_3)_2$
39			CH_2Ph
40	CH_2	H	$CH(CH_3)_2$

Compounds	X	R_1	R_2
41	S	H	CH_3
42			$CH(CH_3)_2$
43			CH_2Ph
44	S	Cl	CH_3
45			$CH(CH_3)_2$
46			CH_2Ph
47	O	H	CH_3
48			$CH(CH_3)_2$
49			CH_2Ph
50	O	Cl	CH_3
51			$CH(CH_3)_2$
52			CH_2Ph
53	CH_2	H	$CH(CH_3)_2$

Reagents and conditions: (a) 3-chloropropionic acid, NaOH, H_2O, reflux, 2-16h; (b) L-aminoacid methyl ester hydrochloride, EDCI, Et_3N, dry CH_2Cl_2, rt, 5-16h; (c) LiOH, THF/H_2O, 0°C-rt, 1h.

Scheme 2. Synthesis of analogues **41-53** and their ester derivatives **28-40**.

A primary screening was performed by HTRF with analogues **13-20** and **41-53**, at a concentration of 400µM, against Syntenin-Syndecan2 complex (GST-S1FL/SDC2) (Table 1).

None of the analogues **13-20** with a spacer length of two atoms displayed a better affinity than fragment **C58** (analogue **16,** inhibition of 56%, IC_{50} of 350 µM). These data revealed the importance of (i) valine as terminal amino acid residue because the corresponding alanine analogue **15** shows an inhibition of 25%, (ii) sulphur atom versus oxygen in the spacer because the corresponding phenoxy analogue **20** exhibits an inhibition of 16%, and (iii) chlorine as *para* substituent because the corresponding non-substituted analogue **14** displays an inhibition of 20%.

Table 1. Inhibition of Syntenin-Syndecan2 complex interaction in the presence of analogues **13-20** and **41-53** at 400 µM confirmed in counter screening experiment using HTRF assay.

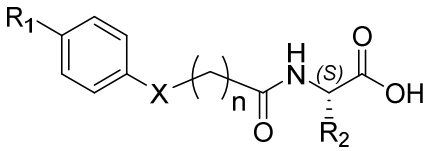

Compounds	X	n	R_1	R_2	% Inhibition affinity GST-S1FL/SDC2
Ctrl	-	-	-	-	0
13	S	1	H	CH_3	0
14				$CH(CH_3)_2$	20
15	S	1	Cl	CH_3	25
16 (C58)				$CH(CH_3)_2$	56
17	O	1	H	CH_3	0
18				$CH(CH_3)_2$	7
19	O	1	Cl	CH_3	0
20				$CH(CH_3)_2$	16
41	S	2	H	CH_3	19
42				$CH(CH_3)_2$	76
43				CH_2Ph	0

44				CH_3	56
45	S	2	Cl	$CH(CH_3)_2$	94
46				CH_2Ph	0
47				CH_3	11
48	O	2	H	$CH(CH_3)_2$	0
49				CH_2Ph	0
50				CH_3	6
51	O	2	Cl	$CH(CH_3)_2$	31
52				CH_2Ph	1
53	CH_2	2	H	$CH(CH_3)_2$	9

Among the analogues **41-53** with a spacer length of three atoms, we identified compound **45** as the most potent inhibitor of syntenin-syndecan-2 interaction, with an inhibition of 94%. As previously, these data revealed the importance of (i) valine as amino acid residue in Cter versus alanine or phenylalanine, (ii) sulphur atom versus oxygen or methylene in the spacer, and (iii) chlorine as *para* substituent. Adding one supplementary methylene group between the sulphur atom and the amide bond resulted in a more than 10-fold improvement of the affinity (IC_{50} = 33 µM and 350 µM for compounds **45** and **C58**, LE = 0.31/LLE = 1.31 and LE = 0.25/LLE = 0.74, respectively). Affinity of compound **45** was validated in the presence of 0.01% NP40 detergent, (IC_{50} = 45 µM and 864 µM for compounds 45 and C58, respectively), demonstrating that its activity is not due to aggregation effect (Figure 2). As reported by Leblanc *et al.*[19] a secondary dose-responses screening confirms the selectivity of analogue **45** for syntenin, with no effect on GRASP/Jam-C and Erbin/P0071 complexes (two other PDZ domains implicated in oncology). Compound **45** was also validated using SPR in an 'orthogonal' validation with K_D values of 130 µM for syntenin-PDZ tandem with C-terminal (data not shown).

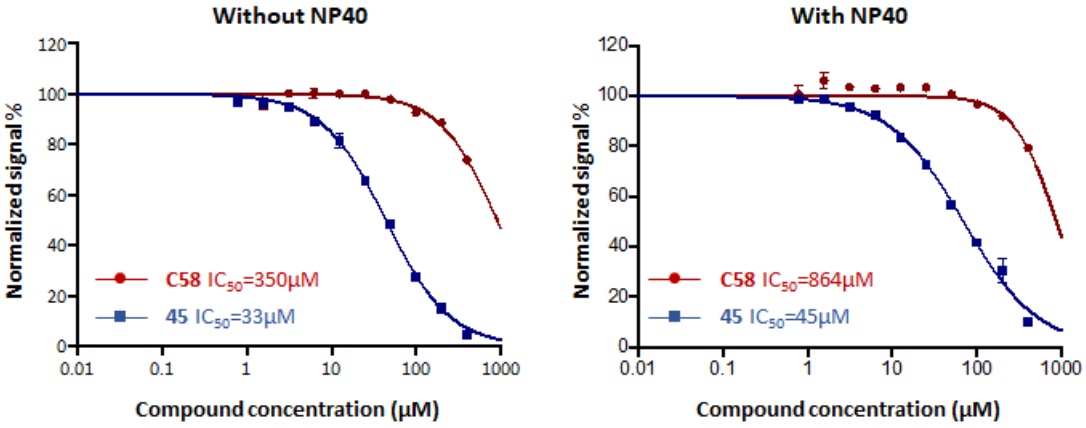

Figure 2. Selectivity profiles and IC_{50} of compounds **C58** (red) and **45** (blue) using HTRF assay without and with 0.01% NP40.

To validate and characterize the binding mode of compound **45**, we soaked it with syntenin crystals. The X-ray crystal structure of **45** bound to syntenin was resolved (PDB code 6RLC) and its binding mode into syntenin PDZ2 domain was confirmed with the expected low strain energy in the carbohydrate spacer (Figure 3). The phenyl ring of **45** exhibits a strong π-stacking with Phe213, its nitrogen atom makes a hydrogen-bonding interaction with the backbone carbonyl of Phe211 and its carboxylic acid forms the expected canonical hydrogen-bonding interactions with backbone amide group of Val209 and Gly210 [19].

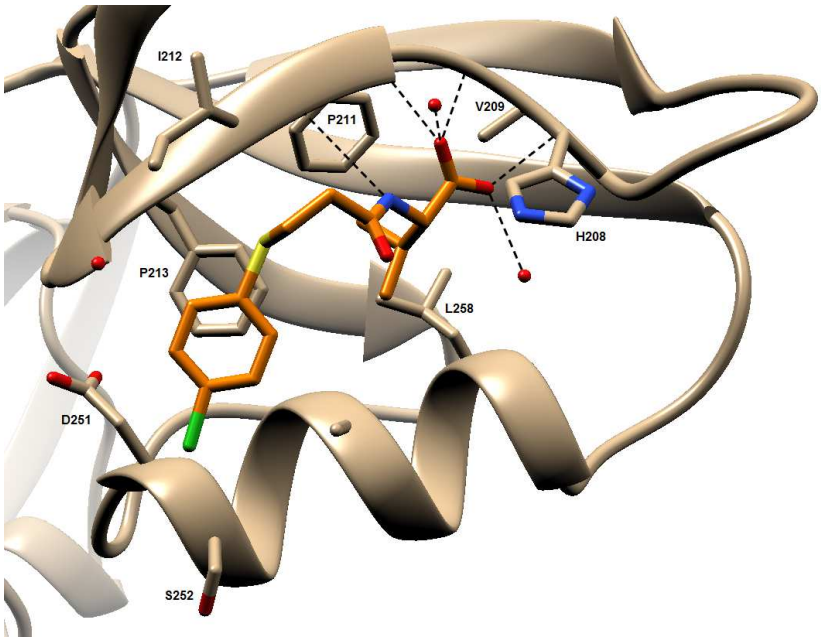

Figure 3. Crystal structure of syntenin PDZ2 domain in complex with compound **45** (PDBID: 6RLC). Compound **45** is displayed in cylinder representation orange carbon atom. Nitrogen, oxygen, chlorine and sulfur are colored in blue, red, green and yellow, respectively. Small red spheres represent water molecules around the binding sites. Hydrogen bond interactions are depicted as black dotted lines. Amino acid residues indicated are those establishing Van der Waals interactions with compound **45**.

Therefore, optimized fragment **45** maintains canonical binding mode and presents a better biological evaluation than the previously identified fragment **C58** (a superimposition view of binding mode of compounds **C58** and **45** with syntenin is given Figure S1B in Supp. Data). For these reasons, we performed the subsequent growing optimization process starting from fragment **45**.

*2-2. Optimization of fragment **45** by fragment growing*

Based on X-ray crystallographic structure of syntenin in complex with fragment **45**, our recently published *in silico* chemistry driven strategy DOTS was applied to the design of optimized

inhibitors [30]. The *in silico* pipeline can be briefly described as follows (see experimental section for details): a focused virtual chemical library was first designed around fragment **45**. The growing strategy consists in exploring the chemical space around this core starting from the logical p-chlorophenyl optimization vector that was naturally included in its structure. Then, the resulting chemical library was virtually screened using the S4MPLE molecular modeling tool [30-32] with constraints on the shared substructure. Constraints were added in the first stage of the simulation to maintain the original binding mode of the fragment, according to the generic growing paradigm in fragment-based drug discovery. In other words, atoms from fragment **45** were constrained while newly added atoms from virtual synthesis were free to explore putative adjacent sub-pockets without any constraints. The goal was to either catch additional interactions in the vicinity of compound **45** or to extend this fragment towards K214, N215, K250 and D251 residues (see illustration in Figure S2 in Supp. Data), because these residues were known to interact with PIP2 ligand in previously published "Syntenin-PDZ-domain/peptide/PIP2" ternary complexes (PDB 4Z33) [33]. However, it is important to mention that these polar and flexible solvent exposed residues do not define a clear druggable sub-pocket. This was confirmed by the FTMap web-server [34], that identifies binding hot spots of macromolecules using *in silico* mapping of small organic probes. It has been proven that regions that can bind clusters of multiple probes correlate with known binding hot spots of macromolecules. Using the Syntenin 4Z33 PDB structure as input, the computational mapping identified 2 main regions within the PDZ2-domain that are predicted to be potential binding hot spots. The first concerns the carboxylate binding loop (V209, G210) and the second is located near Phe213. It should be noted that both regions perfectly match the interaction residues with fragment **45** and bound peptide. However, no particular binding hot spots regions were predicted for K214, N215, K250 and D251 residues. The FTMap simulation confirmed that this PIP2-binding area was not a well-defined druggable sub-pocket (see Figure S2 in Supp. Data).

The final selection of compounds was achieved after visual inspection of the top100 best poses with a focus on compounds that were predicted to interact with previously listed residues. In the end, ten compounds were selected using Suzuki-Miyaura coupling reaction (Table 2).

Table 2. 2D structure of selected compounds by the virtual growing strategy. Building blocks used to build the compounds are depicted with reactive groups (boronic acid or ester) leading to aromatic-carbon bonds highlighted in red.

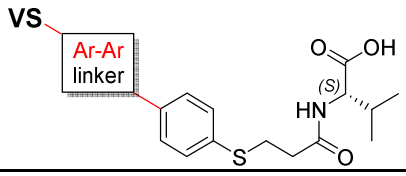

VS ID	Substructure	VS ID	Substructure
VS01	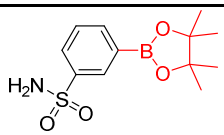	VS06	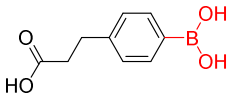
VS02	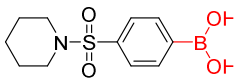	VS07	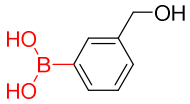
VS03	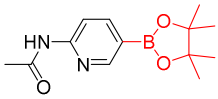	VS08	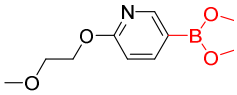
VS04	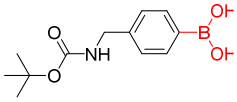	VS09	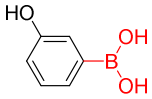
VS05	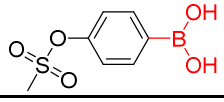	VS10	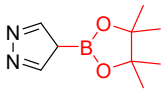

At this stage, we focused on the synthesis of biaryl compounds reported in Table 2, and we decided to explore a strategy using a Suzuki-Miyaura coupling reaction that would allow more flexibility in introducing a large diversity of functionalities. To improve the coupling, we set up a general procedure starting with a 4-bromophenyl intermediate (more reactive substrate than 4-chlorophenyl derivatives depicted in Scheme 1) to generate the selected library. As previously described, 4-bromothiophenol was converted to 3-(4-bromophenylthio)propanoic

acid **55** by S-alkylation with 3-chloropropionic acid under alkaline conditions with excellent yield (Figure 4A) [26, 27]. Compound **55** was condensed with L-valine methyl ester hydrochloride in the presence of EDCI yielded the desired 4-bromophenyl intermediate **56** [28, 29]. To compare the effect of halogens (Br *vs* Cl, analogue **45**) as *para* substituent, intermediate **56** was hydrolysed with LiOH to give derivative **57** [25]. Then, we turned to substitution of the bromo group at the C4-position under standard Suzuki-Miyaura conditions in the presence of $Pd(PPh_3)_4$ under aqueous basic conditions [35]. After few reaction optimization such as performing the reaction with phenylboronic acid and **56** using different bases (sodium, potassium or cesium carbonate) in various solvents such toluene, THF, 1,4-dioxane or ethanol, we were able to conclude that use of $Pd(PPh_3)_4$ (5 mol%) and aqueous Na_2CO_3 in a mixture toluene/ethanol (4/1) at reflux temperature achieved optimum yield (reactions monitored by LC/MS analysis). Furthermore, under these conditions, we noticed that the cross-coupled product is hydrolyzed to the corresponding carboxylic acid derivative, probably due to methyl ester sensitivity to basic hydrolysis. Therefore, intermediate **56** reacted readily with boronic acids **VS02, VS04-07** and **VS-09** as well as boronic esters **VS01**, **VS03** and **VS08** in the presence of $Pd(PPh_3)_4$ and K_2CO_3 in refluxing aqueous toluene/ethanol mixture for 18h providing the corresponding carboxylic acid derivatives **58-66** with good to moderate yields (Figure 4A).

Despite several attempts in different reaction conditions, intermediate **56** failed to react with the commercial pyrazole boronic ester **VS10** (see Table 2). The nitrogen-rich heterocycle here could act as a ligand causing side reactions.

A

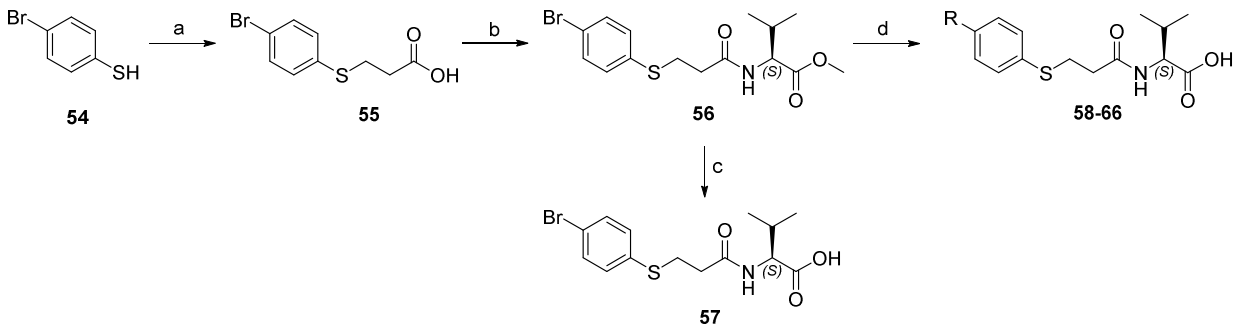

Reagents and conditions: (a) 3-chloropropanoic acid, NaOH, H_2O, reflux, 16h; (b) L-valine methyl ester hydrochloride, EDCI, Et_3N, dry CH_2Cl_2, rt, 16h; (c) LiOH, THF/H_2O, 0°C-rt, 1h; (d) Boronic acid or ester derivative, $Pd(PPh_3)_4$, aqNa_2CO_3, toluene/EtOH, reflux, 18h.

B

Compound	R	IC_{50} (µM)	LE	Compound	R	IC_{50} (µM)	LE
57	Br	47 (51)[a]	0.30 (0.29)[a]	**62**	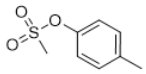	7.5 (204)[a]	0.23 (0.17)[a]
58	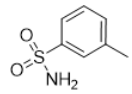	78	0.19	**63**	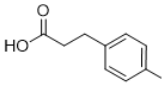	>200	<0.17
59	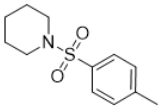	> 200	<0.15	**64**	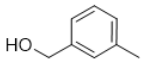	96	0.20
60	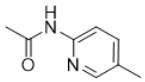	177	0.18	**65**	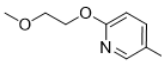	112	0.18
61	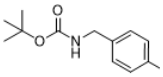	69	0.17	**66**	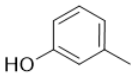	>200	0.19

Figure 4. A. General scheme for synthesis of derivatives **57** and **58-66** *via* Suzuki-Miyaura coupling. **B**. Structure, IC_{50} and LE values of analogues **57-66** on Syntenin-Syndecan2 complex HTRF assay. (a) in parenthesis IC_{50} and LE values with NP40 0.01%. Additional physicochemical efficiency metrics are shown Table S1 in Supp. Data.

The newly synthetized derivatives **57-66** were then evaluated for inhibitory activity on Syntenin-Syndecan2 complex through HTRF assay. Compounds **57** and **62** displayed the lowest IC_{50} values, 47 µM and 7.5 µM respectively (Figure 4B). Analogue **57** corresponds to

the brominated version of **45** (Br *vs* Cl, as *para* substituent) and analogue **62** contains a phenyl ring substituted in *para* position with a methyl mesylate instead of chlorine.

Compounds **45**, **57** and **62** were investigated using cellular assays. We observed an unusual MCF7 exosomes secretion profile after treatment with compound **62** suggesting a tendency to aggregate (see Figure S3 in Supp. Data). For these reasons, IC_{50} values for compounds **57** and **62** were also evaluated in presence of 0.01% NP40 detergent to eliminate potential false positive due to aggregation effects in bioassays. IC_{50} value was not significantly affected by the detergent for compound **57** (51 µM and 47 µM, without and with detergent, respectively). However, IC_{50} value for compound **62** increased to 204 µM in the presence of NP40 (Figure 4B). The goal of our growing strategy was to target residues K214, N215, K250, D251 and S252 residues, because they were either residues in the nearby environment of original fragment or residues involved in binding of the PIP2 ligand in 4Z33 ternary complex. However, the growing stage failed to identify any compound with an improved affinity compared to compound **45** (Figure 4B). Since no better compound was identified using the first small growing round and that targeted residues were not predicted to represent some well-defined pocket, the growing approach was stopped at this stage. In the end, compounds **45** and **57** are the two most potent inhibitors in our study.

Subsequently, exosomal fractions released by MCF7 breast cancer cells treated with compounds **45** and **57** (and their corresponding methyl esters **32** and **56** used as controls) were then analysed by western blot, investigating their effect on both syntenin-dependent and -independent exosomal markers (Figure 5A).

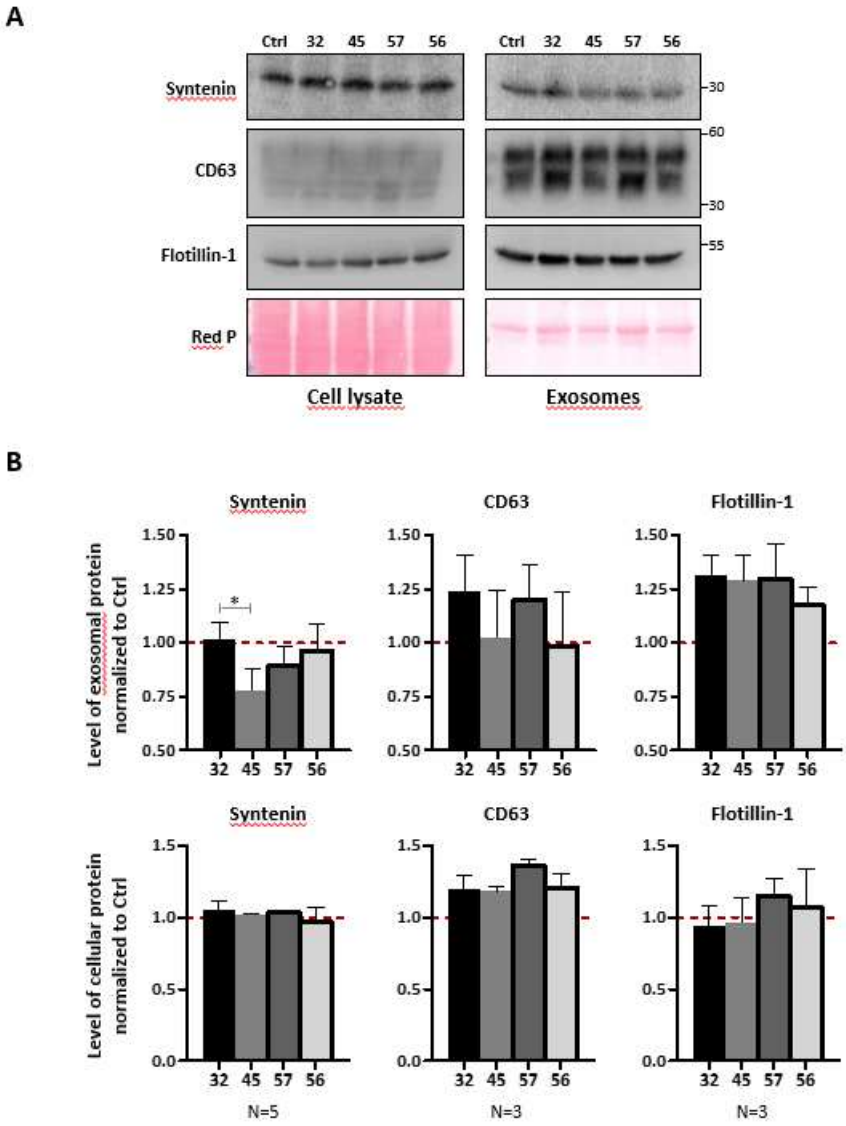

Figure 5. MCF-7 cells were treated with vehicle (Ctrl) or the indicated compound (**32**, **45**, **56** & **57**; 100µM) in medium containing exosome-depleted FCS (10%) for 16h. **A**. Exosomes and corresponding total cell lysates were analyzed by western blot, tracing different markers, as indicated. **B.** Histograms represent mean signal intensities (±SEM) in exosomes, relative to controls (Ctrl). Data were obtained from N independent experiments, as indicated. Statistical analysis was performed using the one-way analysis of variance (ANOVA) with a Tukey posttest.

The amounts of exosomal syntenin were significantly decreased when cells were treated with with 100 µM of compound **45**, but not with 100 µM of **C58** [19] or the inactive compound **32** (ester analogue of **45** used as control, Figure 5A & 5B). On the other hand, compound **57** exhibits a tendency to decrease the amounts of exosomal syntenin, but not its negative control **56** (Figure 5A & 5B). Consistent with our previous study [19], CD63 and the syntenin-independent exosomal marker Flotillin-1 remained unaffected regardless of the treatment (Figure 5A & 5B). As expected, the different treatments do not alter the cellular levels (Figure 5A & 5B).

3- Conclusion

We established a FBDD process against syntenin-syndecan interactions based on a structure-guided optimization strategy. Initial fragment hit **C58** identified by HTRF screening was an attractive starting point for inhibitory design. X-ray crystallographic structures and computational docking were used to guide the fragment growing and allowed the synthesis of the first selective syntenin-PDZ2 inhibitors. Investigations into their capacity to control exosomal pathways validate syntenin-PDZ2 as a promising therapeutic target for inhibiting oncogenic processes and could pave the way for effective therapies for primary tumors and metastasis in the future.

4- Experimental section

4-1. Chemistry

All commercial reagents and solvents were purchased from Sigma Aldrich, Fisher Scientific or Fluorochem companies. Furthermore, all dry solvents were obtained via Sigma Aldrich with Sure/Seal™ system and regular solvents were obtained via Sigma Aldrich at technical grade. Analytical thin layer chromatographiy (TLC) of the reactions was performed on silica gel 60F

254 aluminium plates (Merck) of 0.2 mm thickness with appropriate solvents. The spots were examined with UV light (λ = 254 nm) and Ninhydrin Spray. Preparative flash column chromatographies were performed using silica gel (Merck) G60 230-240 under compressed air. The ^{1}H NMR and ^{13}C NMR spectra were determined with a BRUCKER AMX 250 MHz or BRUKER Avance III nanobay 400 MHz. The chemical shifts are reported in ppm and coupling constants (*J*) are reported in hertz. Reaction monitoring and purity of compounds were recorded by using analytical Agilent Infinity high performance liquid chromatography (Column Zorbax SB-C18 1.8 µM (2.1x50 mm); Mobile phase (A: 0.1% FA H_2O, B: 0.1% FA CH_3CN, Time/%B: 0/10, 4/90, 7 /90, 9/10, 10/10); Flow rate 0.3 mL/min with DAD at 254 nM. All tested compounds yielded data consistent with a purity of ≥ 95%. Low-resolution mass spectra were obtained with Agilent SQ G6120B mass spectrometer in positive and/or negative electrospray modes. Resolution Mass Spectra (HRMS) were obtained on a SYNAPT G2-S WATERS mass spectrometer.

4-1-1. General procedure for the synthesis of methyl propanoate and butanoate intermediates ***5-12***

To a stirred solution of L-aminoacid methyl ester hydrochloride (Alanine or Valine) (4 eq, 4.0 mmol) and triethylamine (5 eq, 5 mmol) in dry dichloromethane was added dropwise the corresponding acetyl chloride derivative (**1-4**) (1 eq, 1.0 mmol) at 4°C. The mixture was stirred under argon atmosphere at 4°C during 1 h then 1-3h at room temperature. After completion, the resulting mixture was washed twice with 1N HCl solution, once with water, once with brine, dried over Na_2SO_4, and evaporated in vacuo. Crude was purified by column chromatography eluting with dichloromethane-methanol (100 to 98:2).

4-1-1-1. (S)-methyl 2-(2-(phenylthio)acetamido)propanoate ***5***

^{1}H NMR ($CDCl_3$, 250 MHz,): δ = 7.29-7.09 (m, 6H), 4.48 (p, *J* = 7.2 Hz, 1H), 3.63 (s, 3H), 3.56 (d, *J* = 0.9 Hz, 2H), 1.25 (d, *J* = 7.2 Hz, 3H). LC/MS (ESI): 252.5 $[M-H]^-$, 254.4 $[M+H]^+$; light brown oil. Yield = 92%.

4-1-1-2. (S)-methyl 3-methyl-2-(2-(phenylthio)acetamido)butanoate ***6***

^{1}H NMR (DMSO-d^6, 400 MHz): δ = 8.39 (bd, *J* = 8.3 Hz, 1H), 7.39-7.35 (m, 2H), 7.34-7.26 (m, 2H), 7.23-7.15 (m, 1H), 4.49 (dd, *J* = 8.3 Hz and 6.2 Hz, 1H), 3.80 (d, *J* = 14.5 Hz, 1H), 3.70 (d, *J* = 14.5 Hz, 1H), 3.63 (s, 3H), 2.02 (m, 1H), 0.85 (d, *J* = 6.8 Hz, 3H), 0.82 (d, *J* = 6.8 Hz, 3H). ^{13}C NMR (DMSO-d^6, 101 MHz): δ = 172.24, 168.76, 136.54, 129.36, 128.30, 126.25, 58.01, 52.21, 36.23, 30.48, 19.33, 18.47; LC/MS (ESI): 280.5 $[M-H]^-$, 282.4 $[M+H]^+$; light yellow oil. Yield = 98%.

4-1-1-3. (S)-methyl 2-(2-(4- chlorophenylthio)acetaamido)propamoate ***7***

^{1}H NMR ($CDCl_3$, 400 MHz): δ = 8.58 (bd, *J* = 7.0 Hz, 1H), 7.38 (bs, 4H), 4.27 (p, *J* = 7.2 Hz, 1H), 3.69 (s, 2H), 3.61 (s, 3H), 1.26 (d, *J* = 7.3 Hz, 3H). ^{13}C NMR ($CDCl_3$, 101 MHz): δ = 173.21, 168.07, 135.65, 131.02, 130.22, 129.25, 52.37, 48.30, 36.46, 17.42; LC/MS (ESI): 286.5 $[M-H]^-$, 288.1 $[M+H]^+$; white solid. Yield = 69%.

4-1-1-4. (S)-methyl 2-(2-(4-chlorophenylthio)acetamido)-3-methylbutanoate ***8***

^{1}H NMR (DMSO-d^6, 400 MHz): δ = 7.21 (bs, 4H), 7.09 (bd, *J* = 8.4 Hz, 1H), 4.43 (dd, *J* = 8.9 Hz and 4.8 Hz, 1H), 3.65 (d, *J* = 16.8 Hz, 1H), 3.63 (s, 3H), 3.55 (d, *J* = 16.8 Hz, 1H), 2.11-1.99 (m, 1H), 0.74 (d, *J* = 6.8 Hz, 3H), 0.73 (d, *J* = 6.9 Hz, 3H). ^{13}C NMR (DMSO-d^6, 101 MHz): δ = 170.87, 166.40, 131.98, 131.94, 128.90, 128.38, 56.33, 51.18, 36.68, 30.15, 17.79, 16.53; LC/MS (ESI): 314.6 $[M-H]^-$, 316.2 $[M+H]^+$; colorless oil. Yield = 90%.

*4-1-1-5. (S)-methyl 2-(2-phenoxyacetamido)propanoate **9***

^{1}H NMR (DMSO-d^6, 400 MHz): δ = 8.50 (bd, *J* = 7.3 Hz, 1H), 7.34-7.26 (m, 2H), 7.00-6.94 (m, 3H), 4.54 (d, *J* = 14.8 Hz, 1H), 4.50 (d, *J* = 14.8 Hz, 1H), 4.39 (p, *J* = 7.3 Hz, 1H), 3.64 (s, 3H), 1.33 (d, *J* = 7.3 Hz, 3H). ^{13}C NMR (DMSO-d^6, 101 MHz): δ = 173.18, 168.13, 158.21, 129.91, 121.64, 115.19, 67.08, 52.40, 47.76, 17.32; LC/MS (ESI): 236.6 $[M-H]^-$, 238.5 $[M+H]^+$; colorless oil. Yield = 74%.

*4-1-1-6. (S)-methyl 3-methyl-2-(2-phenoxyacetamido)butanoate **10***

^{1}H NMR (DMSO-d^6, 400 MHz): δ = 8.28 (bd, *J* = 8.3 Hz, 1H), 7.35-7.25 (m, 2H), 6.95 (m, 3H), 4.62 (d, *J* = 14.7 Hz, 1H), 4.58 (d, *J* = 14.7 Hz, 1H), 4.43 (dd, *J* = 8.3 Hz and 6.4 Hz, 1H), 3.65 (s, 3H), 2.16-1.98 (m, 1H), 0.88 (d, *J* = 6.8 Hz, 3H), 0.86 (d, *J* = 6.8 Hz, 3H). ^{13}C NMR (DMSO-d^6, 101 MHz): δ = 172.22, 168.50, 158.27, 129.90, 121.54, 115.03, 66.80, 57.60, 52.25, 30.30, 19.42, 18.67; LC/MS (ESI): 264.7 $[M-H]^-$, 266.5 $[M+H]^+$; colorless oil. Yield = 63%.

*4-1-1-7. (S)-methyl 2-(2-(4-chlorophenoxy)acetamido)propanoate **11***

^{1}H NMR ($CDCl_3$, 250 MHz): δ = 7.20 (d, *J* = 9.1 Hz, 2H), 6.99 (bd, *J* = 6.7 Hz, 1H), 6.80 (d, *J* = 9.1 Hz, 2H), 4.50 (m, 1H), 4.40 (s, 2H), 3.69 (s, 3H), 1.38 (d, *J* = 7.2 Hz, 3H). LC/MS (ESI): 270.5 $[M-H]^-$, 272.2 $[M+H]^+$; colorless oil. Yield = 89%.

*4-1-1-8. (S)-methyl 2-(2-(4-chlorophenoxy)acetamido)-3-methylbutanoate **12***

^{1}H NMR (DMSO-d^6, 400 MHz): δ = 8.33 (bd, *J* = 8.2 Hz, 1H), 7.34 (d, *J* = 9.1 Hz, 2H), 6.96 (d, *J* = 9.1 Hz, 2H), 4.64 (d, *J* = 14.7 Hz, 1H), 4.59 (d, *J* = 14.7 Hz, 1H), 4.23 (dd, *J* = 8.2 Hz and 6.4 Hz, 1H), 3.65 (s, 3H), 2.14-1.98 (m, 1H), 0.88 (d, *J* = 6.8 Hz, 3H), 0.86 (d, *J* = 6.8 Hz,

3H). ^{13}C NMR (DMSO-d^6, 101 MHz): δ = 172.19, 168.21, 157.19, 129.63, 125.24, 116.86, 67.07, 57.65, 52.25, 30.27, 19.42, 18.70; LC/MS (ESI): 298.5 $[M-H]^-$, 300.1 $[M+H]^+$; colorless oil. Yield = 93%.

*4-1-2. General procedure for the synthesis of amino acid derivatives **13-20**, **41-53** and **57.***

To a stirred solution of ester intermediate derivative (**5-12**, **28-40** or **56**) (1eq, 0.5 mmol) in THF at 0°C, aqueous solution of LiOH (10 eq, 5.0 mmol) was added dropwise. The resulting mixture was stirred 1 h at room temperature. After completion, THF was removed in vacuo. Then, 1N HCl solution was added dropwise until pH 2-3 and the aqueous layer was extracted with ethyl acetate. The organic layer was washed once with water, once with brine, dried over Na_2SO_4, and evaporated in vacuo to afford either a crude residue which does not requires further purification or a crude which was purified by column chromatography eluting with dichloromethane-methanol (95:5).

*4-1-2-1. (S)-2-(2-(phenylthio)acetamido)propanoic acid **13***

^{1}H NMR (DMSO-d^6, 250 MHz): δ = 12.69 (bs, 1H), 8.49 (d, *J* = 7.2 Hz, 1H), 7.42-7.26 (m, 4H), 7.19 (t, *J* = 7.0 Hz, 1H), 4.24 (p, *J* = 7.1 Hz, 1H), 3.72 (s, 2H), 1.28 (d, *J* = 7.3 Hz, 3H). ^{13}C NMR (DMSO-d^6, 63 MHz): δ = 173.88, 167.63, 136.15, 128.86, 127.82, 125.73, 47.76, 36.02, 17.19; LC/MS (ESI): 238.6 $[M-H]^-$, 240.4 $[M+H]^+$; beige solid. Yield = 77%.

*4-1-2-2. (S)-3-methyl-2-(2-(phenylthio)acetamido)butanoic acid **14***

^{1}H NMR (DMSO-d^6, 300 MHz): δ = 12.66 (bs, 1H), 8.19 (d, *J* = 8.6 Hz, 1H), 7.39-7.35 (m, 2H), 7.3-7.25 (m, 2H), 7.22-7.14 (m, 1H), 4.16 (dd, *J* = 8.6 Hz and 5.5 Hz, 1H), 3.81 (d, *J* = 14.5 Hz, 1H), 3.71 (d, *J* = 14.5 Hz, 1H), 2.03 (m, 1H), 0.84 (d, *J* = 6.4 Hz, 3H), 0.82 (d, *J* = 6.4

Hz, 3H). ^{13}C NMR (DMSO-d^6, 75 MHz): δ = 173.20, 168.52, 136.62, 129.34, 128.27, 126.18, 57.82, 36.37, 30.47, 19.47, 18.23; LC/MS (ESI): 266.6 $[M-H]^-$, 268.3 $[M+H]^+$; beige solid. Yield = 88%.

4-1-2-3. (S)-2-(2-(4- chlorophenylthio)acetaamido)propamoic acid ***15***

^{1}H NMR (DMSO-d^6, 300 MHz): δ = 12.56 (bs, 1H), 8.43 (d, *J* = 7.2 Hz, 1H), 7.39 (d, *J* = 8.9 Hz, 2H), 7.34 (d, *J* = 8.8 Hz, 2H), 4.20 (p, *J* = 7.3 Hz, 1H), 3.69 (s, 3H), 1.25 (d, *J* = 7.3 Hz, 3H). ^{13}C NMR (DMSO-d^6, 75 MHz): δ = 174.24, 167.85, 135.75, 130.96, 130.20, 129.22, 48.28, 36.59, 17.70; LC/MS (ESI): 272.5 $[M-H]^-$, 274.1 $[M+H]^+$; white solid. Yield = 78%.

4-1-2-4. (S)-2-(2-(4-chlorophenylthio)acetamido)-3-methylbutanoic acid ***16***

^{1}H NMR (DMSO-d^6, 300 MHz): δ = 12.04 (bs, 1H), 8.06 (d, *J* = 8.5 Hz, 1H), 7.21 (d, *J* = 8.6 Hz, 2H), 7.15 (d, *J* = 8.7 Hz, 2H), 3.96 (dd, *J* = 8.5 Hz and 5.5 Hz, 1H), 3.64 (d, *J* = 14.5 Hz, 1H), 3.53 (d, *J* = 14.5 Hz, 1H), 1.98-1.70 (m, 1H), 0.85-0.53 (m, 6H). ^{13}C NMR (DMSO-d^6, 75 MHz): δ = 172.63, 167.91, 135.26, 130.39, 129.58, 128.71, 57.31, 35.85, 29.92, 18.96, 17.74; LC/MS (ESI): 300.1 $[M-H]^-$, 302.1 $[M+H]^+$; HRMS (TOF, ESI-) cald for $C_{13}H_{15}NO_3SCl$ $[M-H]^-$ 300.0467, found 360.0462; LC/MS (ESI): 300.1 $[M-H]^-$, 302.1 $[M+H]^+$; white solid. Yield = 96%.

4-1-2-5. (S)-2-(2-phenoxyacetamido)propanoic acid ***17***

^{1}H NMR (DMSO-d^6, 300 MHz): δ = 12.62 (bs, 1H), 8.27 (d, *J* = 7.4 Hz, 1H), 7.34-7.26 (m, 2H), 7.02-6.93 (m, 3H), 4.48 (s, 2H), 4.31 (p, *J* = 7.3 Hz, 1H), 1.31 (d, *J* = 7.3 Hz, 3H). ^{13}C NMR (DMSO-d^6, 75 MHz): δ = 174.21, 167.88, 158.23, 129.90, 121.63, 115.22, 67.17, 47.72, 17.61; LC/MS (ESI): 222.8 $[M-H]^-$, 224.4 $[M+H]^+$; white solid. Yield = 78%.

4-1-2-6. (S)-3-methyl-2-(2-phenoxyacetamido)butanoic acid ***18***

^{1}H NMR (DMSO-d^6, 300 MHz): δ = 12.68 (bs, 1H), 7.99 (d, *J* = 8.4 Hz, 1H), 7.35-7.24 (m, 2H), 7.00-6.91 (m, 3H), 4.59 (s, 2H), 4.22 (dd, *J* = 8.5 Hz and 5.7 Hz, 1H), 2.10 (m, 1H), 0.88 (d, *J* = 6.7 Hz, 3H), 0.86 (d, *J* = 6.7 Hz, 3H). ^{13}C NMR (DMSO-d^6, 75 MHz): δ = 173.11, 168.25, 158.26, 129.91, 121.57, 115.08, 66.95, 57.33, 30.38, 19.54, 18.37; LC/MS (ESI): 250.7 $[M-H]^-$, 252.4 $[M+H]^+$; white solid. Yield = 45%.

4-1-2-7. (S)-2-(2-(4-chlorophenoxy)acetamido)propanoic acid ***19***

^{1}H NMR (DMSO-d^6, 250 MHz): δ = 12.72 (bs, 1H), 8.40 (d, *J* = 7.3 Hz, 1H), 7.35 (d, *J* = 8.7 Hz, 2H), 7.01 (d, *J* = 8.8 Hz, 2H), 4.42 (s, 2H), 4.32 (p, *J* = 7.0 Hz, 1H), 1.34 (d, *J* = 7.2 Hz, 3H). ^{13}C NMR (DMSO-d^6, 63 MHz): δ = 171.33, 164.71, 154.09, 126.68, 122.38, 113.99, 64.34, 44.79, 14.56; LC/MS (ESI): 256.5 $[M-H]^-$, 258.3 $[M+H]^+$; white solid. Yield = 95%.

4-1-2-8. (S)-2-(2-(4-chlorophenoxy)acetamido)-3-methylbutanoic acid ***20***

^{1}H NMR ($CDCl_3$, 300 MHz): δ = 7.21 (d, *J* = 9.0 Hz, 2H), 6.92 (bd, *J* = 8.8 Hz, 1H), 6.82 (d, *J* = 8.9 Hz, 2H), 4.23 (dd, *J* = 8.8 Hz and 4.7 Hz, 1H), 4.47 (s, 1H), 2.27-2.13 (m, 1H), 0.91 (d, *J* = 6.9 Hz, 3H), 0.87 (d, *J* = 6.9 Hz, 3H). ^{13}C NMR ($CDCl_3$, 101 MHz): δ = 174.28, 167.45, 154.65, 128.71, 126.37, 115.14, 66.53, 55.61, 29.97, 17.99, 16.54; LC/MS (ESI): 284.5 $[M-H]^-$, 285.9 $[M+H]^+$; white solid. Yield = 85%.

4-1-2-9. (S)-2-(3-phenylthio)propanamido)propamoic acid ***41***

^{1}H NMR (DMSO-d^6, 250 MHz): δ = 12.59 (bs, 1H), 8.31 (d, *J* = 7.2 Hz, 1H), 7.39 (bd, *J* = 4.3 Hz, 4H), 7.26 (dd, *J* = 8.7 Hz and *J* = 4.3 Hz, 1H), 4.25 (p, *J* = 7.3 Hz, 1H), 3.18 (t, *J* = 7.3 Hz, 2H), 2.50 (t, *J* = 7.3 Hz, 2H), 1.30 (d, *J* = 7.3 Hz, 3H); ^{13}C NMR (DMSO-d^6, 101 MHz): δ = 174.59, 170.34, 136.45, 129.55, 128.64, 126.20, 47.94, 35.18, 28.44, 17.69 ; LC/MS (ESI):

252.6 $[M-H]^-$, 254.3 $[M+H]^+$; HRMS (TOF, ESI+) cald for $C_{12}H_{16}NO_3S$ $[M+H]^+$ 254.0851, found 254.0851; white powder. Yield = 93%.

4-1-2-10. (S)-3-methyl-2-(3-phenylthio)propanamido)butanoic acid ***42***

^{1}H NMR (DMSO-d^6, 250 MHz): δ = 12.67 (bs, 1H), 8.17 (d, *J* = 8.6 Hz, 1H), 7.39 (bd, *J* = 4.5 Hz, 4H), 7.26 (dd, *J* = 8.6 Hz and *J* = 4.4 Hz, 1H), 4.23 (dd, *J* = 8.5 and *J* = 5.9 Hz, 1H), 3.19 (t, *J* = 7.2 Hz, 2H), 2.60 (t, *J* = 7.2 Hz, 2H), 2.16-2.01 (m, 1H), 0.93 (bd, *J* = 5.7 Hz, 6H); ^{13}C NMR (DMSO-d^6, 63 MHz): δ = 172.75, 170.32, 136.16, 128.97, 128.56, 125.78, 57.28, 34.97, 29.88, 28.67, 19.04, 18.05 ; LC/MS (ESI): 280.6 $[M-H]^-$, 282.3 $[M+H]^+$; HRMS (TOF, ESI+) cald for $C_{14}H_{20}NO_3S$ $[M+H]^+$ 282.1164, found 282.1165; white solid. Yield = 96%.

4-1-2-11. (S)-3-phenyl-2-(3-phenylthio)propanamido)propamoic acid ***43***

^{1}H NMR (DMSO-d^6, 250 MHz): δ = 12.72 (bs, 1H), 8.24 (d, *J* = 8.1 Hz, 1H), 7.31-7.10 (m, 10H), 4.37 (td, *J* = 9.2 Hz and *J* = 5.0 Hz, 1H), 3.04-2.93 (m, 3H), 2.78 (dd, *J* = 13.7 Hz and *J* = 9.4 Hz, 1H), 2.34 (t, *J* = 7.3 Hz, 2H) ; ^{13}C NMR (DMSO-d^6, 63 MHz): δ = 172.67, 169.98, 137.62, 136.04, 129.05, 128.97, 128.53, 128.05, 126.29, 125.79, 53.39, 36.96, 35.04, 28.46 ; LC/MS (ESI): 328.5 $[M-H]^-$, 330.3 $[M+H]^+$; HRMS (TOF, ESI+) cald for $C_{18}H_{20}NO_3S$ $[M+H]^+$ 330.1164, found 330.1165; white solid. Yield = 49%.

4-1-2-12. (S)-2-(3-(4-cholorophenylthio)propanamido)propamoic acid ***44***

^{1}H NMR ($CDCl_3$, 250 MHz): δ = 7.28-7.14 (m, 4H), 6.17 (bd, *J* = 7.0 Hz, 1H), 4.51 (p *J* = 7.1 Hz, 1H), 3.12 (t, *J* = 7.2 Hz, 2H), 2.45 (t, *J* = 7.2 Hz, 2H), 1.38 (d, *J* = 7.2 Hz, 3H) ; ^{13}C NMR ($CDCl_3$, 63 MHz): δ = 207.45, 170.05, 133.02, 131.95, 130.52, 128.30, 47.29, 35.12, 28.86, 17.02 ; LC/MS (ESI): 286.5 $[M-H]^-$, 288.1 $[M+H]^+$; HRMS (TOF, ESI+) cald for $C_{12}H_{15}NO_3SCl$ $[M+H]^+$ 288.0461, found 288.0461; white solid. Yield = 85%.

4-1-2-13. (S)-2-(3-(4-chlorophenylthio)propanamido)-3-methylbutanoic acid ***45***

^{1}H NMR (DMSO-d^6, 300 MHz): δ = 12.51 (bs, 2H), 8.04 (d, *J* = 8.5 Hz, 1H), 7.38 (d, *J* = 9.2 Hz, 2H), 7.34 (d, *J* = 9.3 Hz, 2H), 4.16 (dd, *J* = 8.4 Hz and 6.0 Hz, 1H), 3.14 (t, *J* = 7.1 Hz, 2H), 2.54 (t, *J* = 7.0 Hz, 2H), 2.03 (m, 1H), 0.87 (bd, *J* = 6.6 Hz, 6H) ; ^{13}C NMR (DMSO-d^6, 75 MHz) δ 173.41, 170.71, 135.69, 130.86, 130.42, 129.40, 57.62, 34.99, 30.34, 28.91, 19.58, 18.48. LC/MS (ESI): 314.6 $[M-H]^-$, 316.2 $[M+H]^+$; HRMS (TOF, ESI+) cald for $C_{14}H_{19}NO_3SCl$ $[M+H]^+$ 316.0774, found 316.0776; white solid. Yield = 89%.

4-1-2-14. (S)-2-(3-(4-cholorophenylthio)propanamido)-3-phenylpropamoic acid ***46***

^{1}H NMR (DMSO-d^6, 250 MHz): δ = 12.82 (bs, 1H), 8.34 (d, *J* = 8.1 Hz, 1H), 7.43 (d, *J* = 8.5 Hz, 2H), 7.35 (d, *J* = 8.7 Hz, 2H), 7.33-7.23 (m, 5H), 4.48 (m, 1H), 3.09 (m, 3H), 2.88 (dd, *J* = 8.4 Hz and 6.0 Hz, 1H), 2.44 (t, *J* = 7.2 Hz, 2H) ; ^{13}C NMR (DMSO-d^6, 63MHz): δ = 172.66, 169.87, 137.60, 135.18, 130.58, 130.19, 129.05, 128.88, 128.06, 126.30, 53.38, 36.98, 34.85, 28.59 ; LC/MS (ESI): 362.6 $[M-H]^-$, 364.1 $[M+H]^+$; HRMS (TOF, ESI+) cald for $C_{18}H_{19}NO_3SCl$ $[M+H]^+$ 364.0774, found 364.0776; white solid. Yield = 97%.

4-1-2-15. (S)-2-(3-(phenoxypropanamido)propanoic acid ***47***

^{1}H NMR (DMSO-d^6, 250 MHz): δ = 12.63 (bs, 1H), 8.35 (d, *J* = 7.3 Hz, 1H), 7.38-7.17 (m, 2H), 7.02-6.84 (m, 3H), 4.27 (p, *J* = 5.8 Hz, 1H), 4.18 (td, *J* = 6.2 Hz and 2.8 Hz, 2H), 2.62 (td, *J* = 6.2 Hz and 1.2 Hz, 2H), 1.30 (d, *J* = 7.3 Hz, 3H). ^{13}C NMR (DMSO-d^6, 63 MHz): δ = ^{13}C NMR (DMSO-d^6, 63 MHz) δ = 173.92, 169.26, 158.48, 130.20, 129.39, 120.57, 116.00, 114.65, 110.85, 64.01, 47.52, 35.18, 17.35; LC/MS (ESI): 236.6 $[M-H]^-$, 238.7 $[M+H]^+$; HRMS (TOF, ESI+) cald for $C_{12}H_{16}NO_4$ $[M+H]^+$ 238.1074, found 238.1079; colorless oil. Yield = 90%.

4-1-2-16. (S)-3-methyl-2-(3-(phenoxypropanamido)butanoic acid ***48***

^{1}H NMR (DMSO-d^6, 250 MHz): δ = 12.70 (bs, 1H), 8.19 (d, *J* = 8.6 Hz, 1H), 7.38-7.20 (m, 2H), 7.00-6.84 (m, 3H), 4.21 (m, 1H), 4.18 (t, *J* = 5.8 Hz, 2H), 2.82-2.58 (m, 2H), 2.16-1.99 (m, 1H), 0.91 (d, *J* = 6.7 Hz, 6H). ^{13}C NMR (DMSO-d^6, 63 MHz): δ = ^{13}C NMR (63 MHz, DMSO) δ = 172.82, 169.80, 158.49, 129.39, 120.55, 114.60, 64.16, 57.18, 35.23, 29.93, 19.04, 18.00; LC/MS (ESI): 264.4 $[M-H]^-$, 266.3 $[M+H]^+$; HRMS (TOF, ESI+) cald for $C_{14}H_{20}NO_4$ $[M+H]^+$ 266.1387, found 266.1395; colorless oil. Yield = 76%.

4-1-2-17. (S)-2-(3-(phenoxypropanamido)-3-phenylpropanoic acid ***49***

^{1}H NMR (DMSO-d^6, 250 MHz): δ = 12.83 (bs, 1H), 8.37 (d, *J* = 8.0 Hz, 1H), 7.36-7.18 (m, 7H), 7.08-6.83 (m, 3H), 4.48 (m, 1H), 4.10 (t, *J* = 6.2 Hz, 2H), 3.09 (dd, *J* = 13.8 Hz and 4.9 Hz, 1H), 2.90 (dd, *J* = 13.8 Hz and 9.3 Hz, 1H), 2.58 (t, *J* = 6.1 Hz, 2H). ^{13}C NMR (DMSO-d^6, 63 MHz): δ = ^{13}C NMR (DMSO-d^6, 63 MHz) δ = 172.73, 169.45, 158.42, 137.61, 129.37, 129.06, 128.06, 126.30, 120.56, 114.60, 63.97, 53.39, 36.92, 35.26; LC/MS (ESI): 312.5 $[M-H]^-$, 314.2 $[M+H]^+$; HRMS (TOF, ESI+) cald for $C_{18}H_{20}N_2O_4$ $[M+H]^+$ 314.1387, found 314.1390; colorless oil. Yield = 75%.

4-1-2-18. (S)-2-(3-(4-chlorophenoxy)propanamido)propanoic acid ***50***

^{1}H NMR (DMSO-d^6, 250 MHz): δ = 8.07 (d, *J* = 7.2 Hz, 1H), 7.13 (d, *J* = 9.0 Hz, 2H), 6.76 (d, *J* = 9.0 Hz, 2H), 4.08-3.92 (m, 3H), 4.00-2.40 (t, *J* = 6.1 Hz, 2H), 1.07 (d, *J* = 7.3 Hz, 3H); ^{13}C NMR (DMSO-d^6, 63 MHz): δ = 174.19, 169.01, 157.36, 129.15, 124.36, 116.44, 64.56, 47.79, 35.10, 17.55 ; LC/MS (ESI): 270.5 $[M-H]^-$, 272.3 $[M+H]^+$; HRMS (TOF, ESI+) cald for $C_{12}H_{15}NO_4Cl$ $[M+H]^+$ 272.0690, found 272.0689; white solid. Yield = 52%.

*4-1-2-19. (S)-2-(3-(4-chlorophenoxy)propanamido)-3-methylbutanoic acid **51***

^{1}H NMR ($CDCl_3$, 250 MHz): δ = 7.16 (d, *J* = 7.6 Hz, 2H), 6.77 (d, *J* = 7.6 Hz, 2H), 6.40 (d, *J* = 8.5 Hz, 1H), 4.55 (dd, *J* = 8.6 Hz and *J* = 4.7 Hz, 1H), 4.17 (t, *J* = 5.6 Hz, 2H), 2.67 (t, *J* = 5.7 Hz, 2H), 2.19 (m, 1H), 0.94-0.85 (m, 6H) ; ^{13}C NMR (DMSO-*d*^{6}, 63 MHz): δ = 172.81, 169.68, 157.34, 129.15, 124.34, 116.37, 64.66, 57.17, 35.07, 29.91, 19.03, 17.99 ; LC/MS (ESI): 298,5 $[M-H]^-$, 300,1 $[M+H]^+$; HRMS (TOF, ESI+) cald for $C_{14}H_{19}NO_4Cl$ $[M+H]^+$ 300.1003, found 300.1003; white solid. Yield = 74%.

*4-1-2-20. (S)-2-(3-(4-chlorophenoxy)propanamido)-3-phenylpropanoic acid **52***

^{1}H NMR (DMSO-*d*^{6}, 250 MHz): δ = 12.85 (bs, 1H), 8.41 (d, *J* = 8.0 Hz, 1H), 7.40-7.26 (m, 7H), 6.94 (d, *J* = 9.0 Hz, 2H), 4.51 (m, 1H), 4.13 (t, *J* = 6.0 Hz, 2H), 3.12 (dd, J = 13.7 Hz and *J* = 4.8 Hz, 1H), 2.93 (dd, *J* = 13.7 Hz and *J* = 9.3 Hz, 1H), 2.60 (t, *J* = 6.0 Hz, 2H) ; ^{13}C NMR (DMSO-*d*^{6}, 63 MHz): δ = 172.72, 169.33, 157.28, 137.61, 129.13, 129.05, 128.06, 126.30, 124.35, 116.38, 64.49, 53.40, 36.91, 35.11; LC/MS (ESI): 346,6 $[M-H]^-$, 348,3 $[M+H]^+$; HRMS (TOF, ESI+) cald for $C_{18}H_{19}NO_4Cl$ $[M+H]^+$ 348.1003, found 348.1006; white solid. Yield = 94%.

*4-1-2-21. (S)-3-methyl-2-(4-(phenylbutanamido)butanoic acid **53***

^{1}H NMR (DMSO-*d*^{6}, 250 MHz): δ = 12.65 (bs, 1H), 8.03 (d, *J* = 8.3 Hz, 1H), 7.36-7.26 (m, 2H), 7.28-7.18 (m, 3H), 4.20 (dd, *J* = 8.1 Hz and *J* = 6.0 Hz, 1H), 2.61 (t, *J* = 7.5 Hz, 2H), 2.25 (t, *J* = 7.3 Hz, 2H), 2.11 (m, 1H), 1.92-1.74 (m, 2H), 0.93 (bd, *J* = 6.7 Hz, 6H) ; ^{13}C NMR (DMSO-*d*^{6},63 MHz): δ = δ 173.01, 172.18, 141.87, 128.24, 128.19, 125.64, 57.20, 34.66, 34.60, 29.72, 27.14, 19.10, 18.10; LC/MS (ESI): 262.6 $[M-H]^-$, 264.4$[M+H]^+$; HRMS (TOF, ESI+) cald for $C_{15}H_{22}NO_3$ $[M+H]^+$ 264.1594, found 264.1590; white solid. Yield = 92%.

4-1-2-22. (S)-2-(3-(4-bromophenylthio)propanamido)-3-methylbutanoic acid ***57***

^{1}H NMR (DMSO-d^6, 250 MHz): δ = 12.67 (bs, 2H), 8.16 (d, *J* = 8.6 Hz, 1H), 7.56 (d, *J* = 8.6 Hz, 2H), 7.33 (d, *J* = 8.6 Hz, 2H), 4.21 (dd, *J* = 8.6 Hz and 5.8 Hz, 1H), 3.20 (t, *J* = 7.1 Hz, 2H), 2.59 (t, *J* = 7.0 Hz, 2H), 2.07 (m, 1H), 0.92 (d, *J* = 6.8 Hz, 3H), 0.93 (d, *J* = 6.8 Hz, 3H). ^{13}C NMR (DMSO-d^6, 63 MHz): δ = 172.96, 170.16, 135.71, 131.74, 129.96, 118.46, 57.04, 34.30, 29.80, 28.05, 19.07, 17.92; LC/MS (ESI): 358.8 $[M-H]^-$ and isotopic peak 360.8, 359.8 $[M+H]^+$ and isotopic peak 361.9; HRMS (TOF, ESI+) cald for $C_{14}H_{19}NO_3SBr$ $[M+H]^+$ 360.0269, found 360.0272; white solid. Yield = 96%.

4-1-3. General procedure for the synthesis of propanoic acid derivatives ***23, 24*** *and* ***55***

To a stirred solution of commercial thiophenol derivative (1 eq, 5.0 mmol) and sodium hydroxide (2.4 eq, 12.0 mmol) in water, aqueous solution of 3-chloropropionic acid was added dropwise (1.7 eq, 8.5 mmol). The mixture was refluxed during 2-16 h. After completion, 1N HCl solution was added dropwise at 4°C until pH 1, to afford a crude precipitate which was filtered and dried. The crude residue does not require further purification.

4-1-3-1. 3-(phenylthio)propanoic acid ***23***

^{1}H NMR ($CDCl_3$, 250 MHz): δ 7.39-7.07 (m, 5H), 3.09 (t, *J* = 7.3 Hz, 2H), 2.61 (t, *J* = 7.3 Hz, 2H). LC/MS (ESI): 181.6 $[M-H]^-$, 183.6 $[M+H]^+$; white powder. Yield = 94%.

4-1-3-2. 3-(4-chlorophenylthio)propanoic acid ***24***

^{1}H NMR ($CDCl_3$, 250 MHz): δ 7.35-7.08 (m, 4H), 3.07 (t, *J* = 7.2 Hz, 2H), 2.59 (t, *J* = 7.2 Hz, 2H). ^{13}C NMR ($CDCl_3$, 63 MHz): δ 175.58, 132.74, 132.16, 130.80, 128.18, 33.13, 28.39. LC/MS (ESI): 215.7 $[M-H]^-$; white powder. Yield = 75%.

*4-1-3-3. 3-(4-bromophenylthio)propanoic acid **55***

^{1}H NMR ($CDCl_3$, 250 MHz): δ 7.35 (d, *J* = 8.4 Hz, 2H), 7.17 (d, *J* = 8.4 Hz, 2H), 3.07 (t, *J* = 7.2 Hz, 2H), 2.60 (t, *J* = 7.2 Hz, 2H). ^{13}C NMR ($CDCl_3$, 63 MHz): δ 178.34, 134.72, 132.79, 132.51, 121.44, 34.68, 29.49. LC/MS (ESI): 259.3 $[M-H]^-$ and isotopic peak 361.4; white solid. Yield = 97%.

*4-1-4. General procedure for the synthesis of amino acid derivatives **28-40** and **56***

To a stirred solution of the corresponding propionic acid derivative (**23-27** or **55**) (1 eq, 1.0 mmol) and L-aminoacid methyl ester hydrochloride (Alanine, Valine or Phenylalanine) (1 eq, 1.0 mmol) in dry dichloromethane, N-Ethyl-N′-(3-dimethylaminopropyl)carbodiimide hydrochloride (2 eq, 2.0 mmol) and triethylamine (2 eq, 2 mmol) were added. The mixture was stirred under argon atmosphere during 5-16 h at room temperature. After completion, the resulting mixture was washed twice with 1N HCl solution, once with water, once with brine, dried over Na_2SO_4, and evaporated in vacuo. Crude was purified by column chromatography eluting with dichloromethane-methanol (100 to 98:2).

*4-1-4-1. (S)-methyl 2-(3-(phenylthio)propanamido)propanoate **28***

^{1}H NMR (DMSO-*d*^{6}, 300 MHz): δ = 8.32 (bd, *J* = 6.8 Hz, 1H), 7.33 (d, *J* = 4.3 Hz, 4H), 7.25-7.14 (m, 1H), 4.27 (p, *J* = 7.2 Hz, 1H), 3.62 (s, 3H), 3.13 (t, *J* = 7.3 Hz, 2H), 2.45 (t, *J* = 7.3 Hz, 2H), 1.26 (d, *J* = 7.3 Hz, 3H). ^{13}C NMR (DMSO-*d*^{6}, 75 MHz): δ 173.52, 170.50, 136.41, 129.54, 128.76, 126.24, 52.26, 48.02, 35.16, 28.51, 17.45; LC/MS (ESI): 266.5 $[M-H]^-$, 268.4 $[M+H]^+$; colorless oil. Yield = 45%.

*4-1-4-2. (S)-methyl 3-methyl-2-(3-(phenylthio)propanamido)butanoate **29***

^{1}H NMR (DMSO-d^6, 400 MHz): δ = 8.24 (bd, *J* = 8.2 Hz, 1H), 7.33 (d, *J* = 4.3 Hz, 4H), 7.24-7.17 (m, 1H), 4.27 (dd, *J* = 8.2 Hz and 6.4 Hz, 1H), 3.63 (s, 3H), 3.13 (t, *J* = 7.2 Hz, 2H), 2.46 (t, *J* = 7.3 Hz, 2H), 2.07-1.90 (m, 1H), 0.88 (d, *J* = 6.8 Hz, 3H), 0.86 (d, *J* = 6.8 Hz, 3H). ^{13}C NMR (DMSO-d^6, 101 MHz): δ = 172.54, 170.99, 136.47, 129.55, 128.70, 126.22, 57.86, 52.10, 35.03, 30.38, 29.32, 28.62, 19.43, 18.73; LC/MS (ESI): 294.6 $[M-H]^-$, 296.1 $[M+H]^+$; colorless oil. Yield = 55%.

4-1-4-3. (S)-methyl 3-phenyl-2-(3-(phenylthio)propanamido)propanoate ***30***

^{1}H NMR (DMSO-d^6, 300 MHz): δ = 8.38 (bd, *J* = 7.7 Hz, 1H), 7.35-7.18 (m, 10H), 4.49 (m, 1H), 3.60 (s, 3H), 3.06-2.99 (m, 3H), 2.88 (dd, *J* = 13.7 Hz and 9.1 Hz, 1H), 2.41 (t, *J* = 7.3 Hz, 2H). ^{13}C NMR (DMSO-d^6, 75 MHz): δ = 172.41, 170.65, 137.62, 136.37, 129.53, 128.73, 128.67, 126.98, 126.23, 54.01, 52.26, 37.22, 35.16, 28.51; LC/MS (ESI): 342.5 $[M-H]^-$, 344.2 $[M+H]^+$; white solid. Yield = 71%.

4-1-4-4. (S)-methyl 2-(3-(4- chlorophenylthio)propanamido)propamoate ***31***

^{1}H NMR (DMSO-d^6, 300 MHz): δ = 8.32 (bd, *J* = 6.8 Hz, 1H), 7.39 (d, *J* = 8.9 Hz, 2H), 7.35 (d, *J* = 9.0 Hz, 2H), 4.26 (p, *J* = 7.3 Hz, 1H), 3.62 (s, 3H), 3.13 (t, *J* = 7.2 Hz, 2H), 2.44 (t, *J* = 7.2 Hz, 2H), 1.25 (d, *J* = 7.3 Hz, 3H). ^{13}C NMR (DMSO-d^6, 75 MHz): δ = 173.49, 170.38, 135.57, 130.90, 130.44, 129.42, 52.26, 48.01, 34.97, 28.63, 17.46; LC/MS (ESI): 301.1 $[M+H]^+$; white solid. Yield = 41%.

4-1-4-5. (S)-methyl 2-(3-(4-chlorophenylthio)propanamido)-3-methylbutanoate ***32***

^{1}H NMR (DMSO-d^6, 300 MHz): δ = 8.19 (bd, *J* = 8.1 Hz, 1H), 7.38 (d, *J* = 8.9 Hz, 2H), 7.35 (d, *J* = 9.0 Hz, 2H), 4.26-4.12 (m, 1H), 3.63 (s, 3H), 3.14 (t, *J* = 7.1 Hz, 2H), 2.53 (t, *J* = 7.1 Hz, 2H), 2.00 (m, 1H), 0.87 (d, *J* = 6.6 Hz, 3H), 0.86 (d, *J* = 6.7 Hz, 3H). ^{13}C NMR (DMSO-

d^6, 75 MHz): δ = 172.47, 170.86, 135.62, 130.89, 130.45, 129.41, 57.87, 52.06, 34.91, 30.39, 28.83, 19.40, 18.72; LC/MS (ESI): 328.63 $[M-H]^-$, 330.1 $[M+H]^+$; white solid. Yield = 62%.

4-1-4-6. (S)-methyl 2-(3-(4-chlorophenylthio)propanamido)-3-phenylpropanoate ***33***

^{1}H NMR (DMSO-*d*^{6}, 300 MHz): δ = 8.38 (bd, *J* = 7.8 Hz, 1H), 7.38 (d, *J* = 8.6 Hz, 2H), 7.31(d, *J* = 8.5 Hz, 2H), 7.28-7.17 (m, 5H), 4.48 (m, 1H), 3.60 (s, 3H), 3.09-2.96 (m, 3H), 2.88 (dd, *J* = 13.7 Hz and 9.2 Hz, 1H), 2.40 (t, *J* = 7.2 Hz, 2H); ^{13}C NMR (DMSO-*d*^{6}, 75 MHz): δ = 172.38, 170.54, 137.59, 135.52, 130.89, 130.42, 129.52, 129.41, 128.68, 126.99, 54.00, 52.26, 37.23, 34.97, 28.64; LC/MS (ESI): 376.5 $[M-H]^-$, 378.1 $[M+H]^+$; white powder. Yield = 54%.

4-1-4-7. (S)-methyl 2-(3-(phenoxypropanamido)propanoate ***34***

^{1}H NMR (DMSO-*d*^{6}, 250 MHz): δ = 8.49 (bd, *J* = 7.0 Hz, 1H), 7.36-7.25 (m, 2H), 6.99-6.90 (m, 3H), 4.33 (p, *J* = 7.3 Hz, 1H), 4.19 (td, *J* = 6.1 Hz and 2.2 Hz, 2H), 3.65 (s, 3H), 2.62 (t, *J* = 6.2 Hz, 2H), 1.31 (d, *J* = 7.3 Hz, 3H). ^{13}C NMR (DMSO-*d*^{6}, 63 MHz): δ = 172.97, 169.45, 158.46, 129.39, 120.58, 114.62, 63.93, 51.69, 47.54, 35.11, 17.05; LC/MS (ESI): 252.5 $[M+H]^+$; colorless oil. Yield = 67%.

4-1-4-8. (S)-methyl 3-methyl-2-(3-(phenoxypropanamido)butanoate ***35***

^{1}H NMR (DMSO-*d*^{6}, 250 MHz): δ = 8.35 (bd, *J* = 8.3 Hz, 1H), 7.35-7.24 (m, 2H), 7.00-6.88 (m, 3H), 4.26 (dd, *J* = 8.2 Hz and 6.5 Hz, 1H), 4.18 (t, *J* = 6.1 Hz, 2H), 3.66 (s, 3H), 2.78-2.59 (m, 2H), 2.06 (m, 1H), 0.93 (d, *J* = 6.6 Hz, 3H), 0.89 (d, *J* = 6.6 Hz, 3H). ^{13}C NMR (DMSO-*d*^{6}, 63 MHz): δ = ^{13}C NMR (63 MHz, DMSO) δ 171.95, 169.96, 158.47, 129.39, 120.56, 114.58, 64.08, 57.40, 51.48, 35.14, 29.96, 22.50, 18.87, 18.20, 15.61; LC/MS (ESI): 280.4 $[M+H]^+$; colorless oil. Yield = 82%.

4-1-4-9. (S)-methyl 2-(3-(phenoxypropanamido)-3-phenyl-propanoate ***36***

^{1}H NMR (DMSO-d^6, 250 MHz): δ = 8.55 (bd, *J* = 7.8 Hz, 1H), 7.35-7.20 (m, 7H), 6.99-6.84 (m, 3H), 4.53 (m, 1H), 4.11 (t, *J* = 6.7 Hz, 2H), 3.63 (s, 3H), 3.12-2.86 (m, 2H), 2.56 (t, *J* = 6.3 Hz, 2H). ^{13}C NMR (DMSO-d^6, 63 MHz): δ = 171.86, 169.63, 158.41, 137.20, 129.38, 129.00, 128.16, 126.45, 120.58, 114.59, 63.90, 53.51, 51.70, 36.85, 35.18; LC/MS (ESI): 328.3 $[M+H]^+$; colorless oil. Yield = 91%.

4-1-4-10. (S)-methyl 2-(3-(4- chlorophenoxy)propanamido)propamoate ***37***

^{1}H NMR (DMSO-d^6, 250 MHz): δ = 8.49 (d, *J* = 7.0 Hz, 1H), 7.35 (d, *J* = 9.1 Hz, 2H), 6.97 (d, *J* = 9.1 Hz, 2H), 4.32 (p, *J* = 7.2 Hz, 1H), 4.18 (td, *J* = 6.1 Hz and *J* = 2.3 Hz, 2H), 3.64 (s, 3H), 2.61 (t, *J* = 6.1 Hz, 2H), 1.30 (d, *J* = 7.3 Hz, 3H); ^{13}C NMR (DMSO-d^6, 63 MHz): δ = 172.95, 169.32, 157.33, 129.16, 124.38, 116.42, 64.46, 51.70, 47.54, 34.96, 17.05; LC/MS (ESI): 286.2 $[M+H]^+$; white powder. Yield = 73%.

4-1-4-11. (S)-methyl 2-(3-(4-chlorophenoxy)propanamido)-3-methylbutanoate ***38***

^{1}H NMR (DMSO-d^6, 250 MHz): δ = 8.12 (d, *J* = 8.3 Hz, 1H), 7.11 (d, *J* = 9.0 Hz, 2H), 6.72 (d, *J* = 9.0 Hz, 2H), 4.02 (dd, *J* = 8.3 Hz and *J* = 6.5 Hz, 1H), 3.95 (t, *J* = 6.1 Hz, 2H), 3.43 (s, 3H), 2.56-2.33 (m, 2H), 1.82 (m, 1H), 0.68 (d, J = 6.7 Hz, 3H), 0.65 (d, J = 6.7 Hz, 3H); ^{13}C NMR (DMSO-d^6, 63 MHz): δ = 171.92, 169.83, 157.33, 129.17, 124.36, 116.37, 64.59, 57.40, 51.49, 34.98, 29.95, 18.87, 18.19; LC/MS (ESI): 314.2 $[M+H]^+$; colorless oil. Yield = 68%.

4-1-4-12. (S)-methyl 2-(3-(4-chlorophenoxy)propanamido)-3-phenyl-propanoate ***39***

^{1}H NMR (DMSO-d^6, 250 MHz): δ = 8.55 (d, *J* = 7.8 Hz, 1H), 7.38-7.22 (m, 7H), 6.91 (d, *J* = 9.0 Hz, 2H), 4.53 (m, 1H), 4.11 (t, *J* = 6.1 Hz, 2H), 3.63 (s, 3H), 3.06 (dd, *J* = 13.7 Hz *J* = 5.5 Hz, 1H), 2.93 (dd, *J* = 13.7 Hz and *J* = 9.2 Hz, 1H), 2.58 (t, *J* = 6.0 Hz, 2H); ^{13}C NMR (DMSO-

d^6, 63 MHz): δ = 171.84, 169.50, 157.27, 137.18, 129.15, 128.99, 128.16, 126.46, 124.37, 116.37, 64.43, 53.50, 51.71, 36.84, 35.03; LC/MS (ESI): 362.2 $[M+H]^+$; %; white powder. Yield = 77%.

4-1-4-13. (S)-methyl 3-methyl-2-(4-(phenylbutanamido)butanoate ***40***

^{1}H NMR (DMSO-*d*^{6}, 250 MHz): δ = 8.15 (d, *J* = 8.0 Hz, 1H), 7.36-7.27 (m, 2H), 7.24-7.17 (m, 3H), 4.19 (dd, *J* = 8.0 Hz and *J* = 6.5 Hz, 1H), 3.65 (s, 3H), 2.59 (t, *J* = 7.6 Hz, 2H), 2.21 (t, *J* = 7.3 Hz, 2H), 2.04 (m, 1H), 1.88-1.75 (m, 2H), 0.91 (d, *J* = 6.8 Hz, 3H), 0.89 (d, *J* = 6.7 Hz, 3H) ; ^{13}C NMR (DMSO-*d*^{6},63 MHz): δ = 172.30, 172.12, 141.81, 128.24, 128.20, 125.66, 57.42, 51.41, 34.61, 34.44, 29.77, 27.02, 18.92, 18.30 ; LC/MS (ESI): 278.4 $[M+H]^+$; colorless oil. Yield = 35%.

4-1-4-14. (S)-methyl 2-(3-(4-bromophenylthio)propanamido)-3-methylbutanoate ***56***

^{1}H NMR ($CDCl_3$, 250 MHz): δ = 7.34 (d, *J* = 8.5 Hz, 2H), 7.15 (d, *J* = 8.5 Hz, 2H), 5.98 (bd, *J* = 8.6 Hz, 1H), 4.50 (dd, *J* = 8.8 Hz and 4.6 Hz, 1H), 3.66 (s, 3H), 3.12 (t, *J* = 7.2 Hz, 2H), 2.45 (td, *J* = 7.2 Hz and 1.6 Hz, 2H), 2.07 (m, 1H), 0.67 (d, *J* = 6.9 Hz, 3H), 0.82 (d, *J* = 6.9 Hz, 3H). ^{13}C NMR ($CDCl_3$, 63 MHz): δ = 170.97, 168.97, 133.05, 130.58, 129.75, 118.83, 55.50, 50.72, 34.40, 29.83, 27.91, 17.42, 16.29; LC/MS (ESI): 372.3 $[M-H]^-$ and isotopic peak 374,4, 374.1 $[M+H]^+$ and isotopic peak 376.1; white solid. Yield = 72%.

4-1-5. General procedure for Suzuki synthesis of valine derivatives ***58-66***

To a solution of compound **56** (1eq, 0.2 mmol), boronic acid or ester derivative (1.5 eq, 0.3 mmol) and $Pd[P(Ph_3)]_4$ (5 mol%) in a mixture toluene/ethanol (2/0.5 mL) was added an aqueous solution of Na_2CO_3 (2 eq, 0.4 mmol, 0.5 mL). The resulting mixture was refluxed under argon atmosphere during 18 h, cooled and then concentrated. To the resulting residue was added

dropwise 1N HCl solution 4°C until pH 1, the aqueous layer was extracted twice with ethyl acetate. The combined organic layers were washed once with water, once with brine, dried over Na_2SO_4, and evaporated under vacuum. Crude was purified by column chromatography eluting with dichloromethane-methanol (98:2 to 80:20).

4-1-5-1. (2S)-3-methyl-2-(3-{[4-(3-sulfamoylphenyl)phenyl]sulfanyl}propanamido)butanoic acid ***58***

^{1}H NMR (CD_3OD, 250 MHz): δ = 8.04 (t, *J* = 1.6 Hz, 1H), 7.75 (m, 2H), 7.52 (d, *J* = 8.6 Hz, 2H), 7.50 (m, 1H), 7.37 (d, *J* = 8.6 Hz, 2H), 4.23 (d, *J* = 5.6 Hz, 1H), 3.15 (t, *J* = 7.2 Hz, 2H), 2.54 (t, *J* = 7.2 Hz, 2H), 2.15-1.96 (m, 1H), 0.88 (d, *J* = 6.7 Hz, 3H), 0.85 (d, *J* = 6.7 Hz, 3H).^{13}C NMR (CD_3OD, 63 MHz δ = 175.26, 173.91, 145.76, 142.62, 138.53, 137.81, 131.31, 131.11, 130.72, 128.64, 125.83, 125.21, 59.30, 36.41, 31.75, 30.03, 19.70, 18.38; LC/MS (ESI): 434.5 $[M-H]^-$, 436.5 $[M+H]^+$; HRMS (TOF, ESI+) cald for $C_{20}H_{25}N_2O_5S_2$ $[M+H]^+$ 437.1205, found 437.1208; purity = 99%; pale yellow solid. Yield = 63%.

4-1-5-2.(2S)-3-methyl-2-[3-({4-[4-(piperidine-1-sulfonyl)phenyl]phenyl}sulfanyl)propanamido]butanoic acid ***59***

^{1}H NMR (DMSO-d^6, 400 MHz): δ = 8.02 (bd, *J* = 8.4 Hz, 1H), 7.93 (d, *J* = 8.5 Hz, 2H), 7.79 (d, *J* = 8.5 Hz, 2H), 7.73 (d, *J* = 8.5 Hz, 2H), 7.45 (d, *J* = 8.5 Hz, 2H), 4.16 (dd, *J* = 8.6 Hz and 5.7 Hz, 1H), 3.48-3.39 (m, 2H), 3.22 (t, *J* = 7.2 Hz, 2H), 2.92 (t, *J* = 5.4 Hz, 4H), 2.10-1.99 (m, 1H), 1.61-1.50 (m, 4H), 1.42-1.34 (m, 2H), 0.88 (d, *J* = 6.8 Hz, 3H), 0.87 (d, *J* = 6.8 Hz, 3H).^{13}C NMR (DMSO-d^6, 101 MHz): δ = 185.40, 170.63, 144.14, 137.81, 135.83, 134.70, 128.68, 128.60, 128.09, 127.56, 57.93, 47.05, 35.12, 30.50, 28.35, 25.19, 23.29, 19.71, 18.53; LC/MS (ESI): 502.7 $[M-H]^-$, 504.6 $[M+H]^+$; HRMS (TOF, ESI+) cald for $C_{25}H_{33}N_2O_5S_2$ $[M+H]^+$ 505.1831, found 505.1833; purity = 98%; light brown solid. Yield = 48%.

4-1-5-3. (2S)-2-(3-{[4-(6-acetamidopyridin-3-yl)phenyl]sulfanyl}propanamido)-3-methylbutanoic acid ***60***

^{1}H NMR (DMSO-d^6, 250 MHz): δ = 10.62 (s, 1H), 8.65 (d, *J* = 1.6 Hz, 1H), 8.17 (d, *J* = 8.8 Hz, 1H), 8.09 (dd, *J* = 8.7 Hz and 2.4 Hz, 1H), 7.86 (bd, *J* = 8.5 Hz, 1H), 7.69 (d, *J* = 8.4 Hz, 2H), 7.43 (d, *J* = 8.4 Hz, 2H), 4.12 (dd, *J* = 8.6 Hz and 5.4 Hz, 1H), 3.20 (t, *J* = 7.1 Hz, 2H), 2.63-2.55 (m, 2H), 2.13 (s, 3H), 2.10-2.00 (m, 1H), 1.42-1.34 (m, 2H), 0.87 (d, *J* = 6.8 Hz, 3H), 0.86 (d, *J* = 6.7 Hz, 3H).^{13}C NMR (DMSO-d^6, 63 MHz): δ = 174.45, 169.86, 169.28, 151.30, 145.43, 135.77, 135.73, 134.09, 130.23, 128.60, 126.82, 113.16, 57.99, 34.83, 30.66, 28.27, 23.89, 19.43, 18.04; LC/MS (ESI): 413.6 $[M-H]^-$, 415.7 $[M+H]^+$; HRMS (TOF, ESI+) cald for $C_{21}H_{26}N_3O_4S$ $[M+H]^+$ 416.1644, found 416.1645; purity = 98%; light orange solid. Yield = 58%.

4-1-5-4. (2S)-2-[3-({4-[4-({[(tert-butoxy)carbonyl]amino}methyl)phenyl]phenyl}sulfanyl)propanamido]-3-methylbutanoic acid ***61***

^{1}H NMR ($CDCl_3$, 250 MHz): δ = 7.47 (d, *J* = 8.2 Hz, 2H), 7.44 (d, *J* = 8.2 Hz, 2H), 7.35 (d, *J* = 8.4 Hz, 2H), 7.28 (d, *J* = 8.2 Hz, 2H), 6.03 (bd, *J* = 8.5 Hz, 1H), 4.83 (bs, 1H), 4.52 (dd, *J* = 8.8 Hz and 4.8 Hz, 1H), 4.28 (bd, *J* = 3.5 Hz, 2H), 3.18 (t, *J* = 7.2 Hz, 2H), 2.49 (t, *J* = 7.2 Hz, 2H), 2.09 (m, 1H), 1.40 (s, 9H), 0.88 (d, *J* = 6.9 Hz, 3H), 0.84 (d, *J* = 6.9 Hz, 3H). ^{13}C NMR (DMSO-d^6, 101 MHz): δ = 170.51, 160.99, 156.29, 139.94, 138.28, 137.82, 135.70, 129.15, 128.03, 127.57, 126.73, 78.27, 58.21, 43.54, 35.33, 30.64, 28.84, 28.73, 19.84, 18.55; LC/MS (ESI): 484.4 $[M-H]^-$, 430.6 $[M-tBu]^+$ and 508.6 $[M+Na]^+$; HRMS (TOF, ESI+) cald for $C_{26}H_{34}N_2O_5SNa$ $[M+H]^+$ 509.2086, found 509.2088; purity = 97%; light brown solid. Yield = 21%.

4-1-5-5. (2S)-2-[3-({4-[4-(methanesulfonyloxy)phenyl]phenyl}sulfanyl)propanamido]-3-methylbutanoic acid ***62***

^{1}H NMR (DMSO-d^6, 250 MHz): δ = 7.82 (bs, 1H), 7.77 (d, *J* = 8.5 Hz, 2H), 7.65 (d, *J* = 8.2 Hz, 2H), 7.43 (d, *J* = 8.5 Hz, 2H), 7.42 (d, *J* = 8.2 Hz, 2H), 4.09 (dd, *J* = 8.1 Hz and 5.3 Hz, 1H), 3.42 (s, 3H), 3.19 (t, *J* = 7.1 Hz, 2H), 2.36 (t, *J* = 6.9 Hz, 2H), 2.06 (m, 1H), 0.86 (d, *J* = 6.4 Hz, 3H), 0.84 (d, *J* = 6.3 Hz, 3H). ^{13}C NMR (DMSO-d^6, 101 MHz): δ = 176.84, 170.21, 148.97, 139.05, 136.63, 136.56, 128.88, 128.52, 127.82, 123.20, 58.69, 37.91, 35.43, 30.91, 28.72, 20.00, 18.58; LC/MS (ESI): 449.6 $[M-H]^-$, 451.5 $[M+H]^+$; HRMS (TOF, ESI+) cald for $C_{21}H_{26}NO_6S_2$ $[M+H]^+$ 452.1202, found 452.1205; purity = 97%; light orange solid. Yield = 42%.

4-1-5-6. (2S)-2-[3-({4-[4-(2-carboxyethyl)phenyl]phenyl}sulfanyl)propanamido]-3-methylbutanoic acid ***63***

^{1}H NMR (CD_3OD, 250 MHz): δ = 7.46 (d, *J* = 8.1 Hz, 2H), 7.43 (d, *J* = 7.8 Hz, 2H), 7.34 (d, *J* = 8.3 Hz, 2H), 7.20 (d, *J* = 8.0 Hz, 2H), 4.21 (bd, *J* = 5.5 Hz, 1H), 3.12 (t, *J* = 7.1 Hz, 2H), 2.85 (t, *J* = 7.7 Hz, 2H), 2.52 (bt, *J* = 7.4 Hz, 4H), 2.06 (m, 1H), 0.88 (d, *J* = 6.7 Hz, 3H), 0.85 (d, *J* = 6.7 Hz, 3H). ^{13}C NMR (DMSO-d^6, 101 MHz): δ = 173.97, 170.61, 140.75, 137.93, 137.62, 135.55, 134.65, 129.34, 129.18, 127.52, 126.77, 58.00, 35.72, 35.32, 30.55, 30.49, 28.85, 19.76, 18.54; LC/MS (ESI): 427.6 $[M-H]^-$, 429.6 $[M+H]^+$; HRMS (TOF, ESI+) cald for $C_{23}H_{28}NO_5S$ $[M+H]^+$ 430.1688, found 430.1690; purity = 95%; white solid. Yield = 30%.

4-1-5-7. (2S)-2-[3-({4-[3-(hydroxymethyl)phenyl]phenyl}sulfanyl)propanamido]-3-methylbutanoic acid ***64***

^{1}H NMR (CD_3OD, 250 MHz): δ = 7.15 (m, 1H), 7.48 (d, *J* = 8.6 Hz, 2H), 7.44-7.38 (m, 1H), 7.35 (d, *J* = 8.6 Hz, 2H), 7.29 (d, *J* = 7.5 Hz, 1H), 7.26-7.19 (m, 1H), 4.57 (s, 2H), 4.20 (bd, *J* = 5.5 Hz, 1H), 3.13 (t, *J* = 7.2 Hz, 2H, 2.53 (t, *J* = 7.2 Hz, 2H), 2.05 (m, 1H), 0.88 (d, *J* = 6.8 Hz, 3H), 0.85 (d, *J* = 6.8 Hz, 3H). ^{13}C NMR (CD_3OD, 63 MHz): δ = 175.10, 173.11, 142.66, 140.98, 139.67, 135.61, 130.24, 129.18, 127.80, 126.27, 125.91, 125.55, 64.40, 58.97, 35.79, 31.02, 29.63, 19.00, 17.62; LC/MS (ESI): 385.6 $[M-H]^-$, 387.7 $[M+H]^+$; HRMS (TOF, ESI-) cald for $C_{21}H_{24}NO_4S$ $[M-H]^-$ 386.1426, found 386.1429; purity = 99%; yellow solid. Yield = 56%.

4-1-5-8. (2S)-2-[3-({4-[6-(2-methoxyethoxy)pyridin-3-yl]phenyl}sulfanyl)propanamido]-3-methylbutanoic acid ***65***

^{1}H NMR (DMSO-d^6, 400 MHz): δ = 8.46 (d, *J* = 2.3 Hz, 1H), 8.00 (dd, *J* = 8.6 Hz and 2.6 Hz, 1H), 7.84 (bd, *J* = 6.6 Hz, 1H), 7.62 (d, *J* = 8.4 Hz, 2H), 7.41 (d, *J* = 8.4 Hz, 2H), 6.91 (d, *J* = 8.7 Hz, 1H), 4.42 (bt, *J* = 4.7 Hz, 2H), 4.11 (dd, *J* = 8.7 Hz and 5.4 Hz, 1H), 3.68 (bt, *J* = 4.7 Hz, 2H), 3.24 (s, 3H), 3.17 (t, *J* = 7.2 Hz, 2H), 2.55 (t, *J* = 7.4 Hz, 2H), 2.12-1.97 (m, 1H), 0.86 (d, *J* = 6.5 Hz, 3H), 0.84 (d, *J* = 6.4 Hz, 3H). ^{13}C NMR (DMSO-d^6, 63 MHz): δ = 174.19, 170.00, 162.54, 144.28, 137.39, 135.32, 134.27, 128.71, 128.64, 126.82, 110.80, 70.19, 64.71, 58.06, 34.85, 30.25, 28.33, 19.39, 18.01; LC/MS (ESI): 430.5 $[M-H]^-$, 432.6 $[M+H]^+$; HRMS (TOF, ESI+) cald for $C_{22}H_{29}N_2O_5S$ $[M+H]^+$ 433.1797, found 433.1801; purity = 98%; light orange solid. Yield = 46%.

4-1-5-9. (2S)-2-(3-{[4-(3-hydroxyphenyl)phenyl]sulfanyl}propanamido)-3-methylbutanoic acid ***66***

^{1}H NMR (CD_3OD, 250 MHz): δ = 7.43 (d, *J* = 8.6 Hz, 2H), 7.33 (d, *J* = 8.6 Hz, 2H), 7.14 (t, *J* = 7.9 Hz, 1H), 6.95 (dm, *J* = 7.7 Hz, 1H), 6.91 (bt, *J* = 2.1 Hz, 1H), 6.66 (ddd, *J* = 8.1 Hz, 2.1

Hz and 1.0 Hz 1H), 4.18 (d, *J* = 5.5 Hz, 1H), 3.12 (t, *J* = 7.2 Hz, 2H), 2.52 (t, *J* = 7.2 Hz, 2H), 2.14-2.00 (m, 1H), 0.88 (d, *J* = 7.1 Hz, 3H), 0.85 (d, *J* = 7.1 Hz, 3H). ^{13}C NMR (CD_3OD, 101 MHz): δ = 175.48, 172.44, 157.57, 141.67, 139.15, 134.84, 129.59, 129.52, 127.11, 117.67, 113.99, 113.16, 58.75, 35.25, 30.44, 29.06, 18.46, 17.06; LC/MS (ESI): 371.6 $[M-H]^-$, 373.7 $[M+H]^+$; HRMS (TOF, ESI-) cald for $C_{20}H_{22}NO_4S$ $[M-H]^-$ 372.1270, found 372.1269; purity = 99%; light brown solid. Yield = 34%.

4-2. HTRF GST-S1FL/SDC2 assay

4-2-1. Production of GST-syntenin full length for HTRF experiments

Competent E.coli (ER2566 strain) cells were transformed with the human syntenin1 pGEX-5X expression vector (GE Healthcare). Expression of N-terminally GST-tagged syntenin-1 full length was induced overnight at 30 °C and by the addition of 0.4mM IPTG (Fisher Scientific). Protein was purified using GSTrap4B columns 28-4017-45 (GE Healthcare).

4-2-2. HTRF screen

HTRF assays were performed in white 96Well Small Volume™HiBase Polystyrene Microplates (Greiner) with a total working volume of 100µL, as described previously [17]. Briefly, compounds were firstly dispensed into the wells at 400µM for the primary screen or with serial DMSO dilutions for IC50 measurement assays. Primary screening assays have been performed in monoplicate while IC50 measurements were performed in triplicates. All HTRF reagents were purchased from CisBio Bioassays and reconstituted according to the supplier protocols. The plates were spin for 3 min at 500g and then incubated at 4°C for 16 h. The HTRF signals were recorded on a POLAR star Omega plate reader (BMG Labtech) with an excitation filter at 337 nm and fluorescence wavelength measurement at 620 and 665 nm, an integration delay of 60µs and an integration time of 400µs. Results were analyzed with a two-wavelength signal ratio: [intensity (665 nm)/intensity (620 nm)]*10^4. Percentage of inhibition was

calculated using the following equation: % inhibition = [(compound signal)-(min signal)]/[(max signal)-(min signal)]*100, where 'max signal' is the signal ratio with the compound vehicle alone (DMSO) and 'min signal' the signal ratio without protein B. For IC50 measurements, values were normalized and fitted with Prism (GraphPad software) using the following equation: Y=100/(1+((X/IC50)^Hill slope)).

4-3. Molecular modeling

4-3-1. Binding site preparation

MOE version 2016 (Chemical Computing Group Inc., Montreal, QC, Canada) was used to prepare the binding sites starting from the X-ray structure of the syntenin PDZ domain in complex with compound **45** (6RLC). All residues, with at least one atom within 14 Å radius from reference fragment were selected to define the binding site. A large binding site was defined because the docking engine (S4MPLE) relies on a FF-based energy function and the goal is to explore adjacent sub-pockets using a growing strategy. Two different binding site files were prepared because both potential orientations of the N215 sidechain (flip of terminal amide) were considered.

4-3-2. Design of virtual library

The creation of the virtual focused library relied on the procedure described in the DOTS methodology [30]. Briefly, a focused library was generated starting from an activated substructure (here, fragment **45** that contains an aryl halide reactive function), a collection of commercially available BBs and a set of *in silico* encoded medicinal chemistry relevant chemical reactions. This chemistry-driven strategy is expected to design accessible compounds with high reaction yields. The single Suzuki rule (#31 according to the reference study [36] was enabled for the design stage. A raw focused library of 1865 compounds was automatically

designed. Then, several fully automated post-processing stages were applied to this raw focused library to extract a subset of duplicate-free compounds with a focus on structures with reasonable physiochemical properties. More precisely, a structural check was performed with StructureChecker from ChemAxon (http://www.chemaxon.com) to eliminate compounds with any structural warning. Duplicates and compounds that contain at least one undesired element (other than C, H, N, O, P, S, F, Cl, Br or I) were also discarded. Usual threshold values for common physico-chemical descriptors (molecular weight ≤ 550, cLogP ≤ 5.5, tPSA ≤ 150 Å², H-Bond acceptors ≤ 10, H-Bond donors ≤ 5, rotational bond count ≤ 14, and formal charge count ≤ 2) were used to automatically extract a subset of compounds with reasonable properties. Then, yuck filters, which were used to design the clean subset of the ZINC database (http://zinc.docking.org), were employed to reject compounds with undesired functional groups. Cxcalc and Jcsearch programs from ChemAxon were respectively used to compute descriptors and detect undesired substructures. The last post-processing stage involved various computations which are required for the subsequent virtual screening: major microspecies, partial charges, force-field atomic types, and single 3D-conformer were computed for each compound. A maximum common substructure (MCS) algorithm was also used to flag atoms that were already present in the fragment **45**. These atoms were constrained in the subsequent virtual screening stage (see below). The mapping of force-field atomic types was done using programs from AmberTools (http://ambermd.org), while all the other steps were performed using in house tools relying on the ChemAxon Java API. In the end, the virtual focused chemical library contained 402 compounds.

4-3-3. Virtual screening

The virtual screening was performed on both prepared binding sites as described in the DOTS methodology [PMID 29883107]. More precisely, the final subset of compounds was screened

using the S4MPLE conformational tool with constraints on the original location of the fragment 45. Unflagged atoms, corresponding to newly added atoms from virtual synthesis, were free to explore adjacent sub-pockets without any constraints. The sampling stage mainly consisted in three independent simulations of 400 generations with a population of 30 individuals. All saved poses were merged into one file before switching to the post-processing stage that involved the minimization of all non-redundant poses while unlocking all ligand atoms. The energy used to rank all screened compounds was equal to the best energy of the complex minus the energy of the best conformer of the free ligand. The latter is obtained by performing three independent simulations with the same parameters on the ligand alone. The goal is to compute a potential energy difference between bound and free forms to estimate the interaction energy while considering the strain energy of the ligand.

4-4. Cellular evaluation

4-4-1. Cell culture and reagents

MCF-7 cell lines were purchased from the American Type culture collection (Manassas, VA). Cells were grown in DMEM-F12 (Invitrogen) supplemented with 10% fetal calf serum (FCS) (Eurobio) at 37°C under 5% CO2. Syntenin CRISPR/Cas9 knockout (SyntKO) MCF-7 cells were generated following the procedures as previously described [37]. Briefly, SDCBP-specific gRNA oligos sgRNASDCBP1 targeting exon1 (F: CACCgCTATCCCTCACGATGGAAGT; R: AAACACTTCCATCGTGAGGGATAGc) were cloned into the pX458 two-in-one CRISPR targeting vector (Addgene, Cambridge, MA), individually transfected into MCF7 cells and sorted for GFP expression after 48h. Single cell clones were grown and screened by western blotting for syntenin expression. One individual clone has been used in the *in vitro* experiments. The cDNA encoding mCherry-syntenin was derived from the eGFP-syntenin cDNA construct, by restriction-ligation. The expression vector for Ce-RAB5(Q79L) was received from W.

Annaert (K.U. Leuven, Belgium). The CAY10594 inhibitor (used at 10 µM) was purchased from Santa Cruz (sc-223874) [19].

4-4-2. Cancer cell viability

The effects of the compounds **C58** and **SyntOFF** were tested both on MCF-7 and MCF-7 SyntKO cells. Briefly, the cells were treated with increasing concentrations of the compounds for 48hours and early/late apoptosis was measured by using the FITC Annexin V apoptosis detection kit with 7-AAD (Biolegend, San Diego, CA) according to the manufacturer. Annexin V positive but 7-AAD negative (early apoptotic cells) and Annexin V positive and 7-AAD positive (late stage apoptosis) was determined by using FACS LSRII flow cytometer (BD Biosciences) and data were analyzed with Flowjo software (Tree Star).

4-4-3. Exosomes and total cell lysates

For comparative analyses, exosome-enriched fractions were collected from equivalent amounts of culture medium, conditioned by equivalent amounts of cells. MCF-7 cells were treated with indicated compounds or with DMSO 0.2% as control, in medium containing exosome-depleted FCS (10%). After 16hours, cell media were collected and exosomes were isolated by three sequential centrifugation steps at 4 °C: 10 min at 500×g, to remove cells; 30 min at 10,000×g, to remove cell debris; and 1h30min at 100,000×g, to pellet exosomes (exosome-enriched fraction), followed by one wash with 1400µL of PBS1X (100,000×g, 1h), to remove soluble serum and secreted proteins. Exosomal pellets were then re-suspended in 100µL of PBS1X. The lysates from corresponding cultures were cleared by centrifugation at 1500rpm for 5 min and then resuspended in lysis buffer (TrisHCL pH 7.4 30mM, NaCl 150mM, 1% NP40 (IGEPAL), 1µg/ml aprotinin, 1µg/ml leupeptin). Although only little variations were observed from sample to sample, exosomal amounts loaded for the western blot were normalized according to the number of parent cells from where exosomes were secreted.

4-4-4. Western blots

The proteins were heat-denaturated in Laemmli sample buffer, fractionated in 12.5% or 15% gels by SDS–PAGE and electro-transferred to nitrocellulose membrane. Membranes were stained with Ponceau red and immunoblotted with the indicated primary antibodies for: CD9 (1/5000), CD63 (1/5000), CD81 (1/5000) and ADAM10 (1/1000) antibodies provided by E. Rubinstein (Université Paris-Sud UMRS_935, Villejuif); syntenin (Homemade; 1/3000), Tubulin (Sigma-Aldrich; 1/10000), ALIX (Homemade, 1/500), HSP70 (Santa Cruz Biotechnology; 1/500), Flotillin-1 (BD Biosciences; 1/1000), EGFR (Cell Signaling; 1/1000), EpCAM (Santa Cruz Biotechnology; 1/200), Fibronectin (BD Biosciences; 1/5000), Src (Cell signaling; 1/1000), TSP1 (Lab Vision; 1/100), SDC1 intracellular domain (Homemade, 1/1000), SDC4 intracellular domain (Abnova; 1/2000), and HRP-conjugated secondary antibodies (Mouse or Rabbit, Thermofisher scientific; 1/10000). Signals were visualized using Amersham ECL Prime Western Blotting Detection Reagent (GE Healthcare) [19].

Acknowledgements

This work was supported by grants from the National Research Agency (ANR, Investissements d'Avenir, A∗MIDEX project ANR-11-IDEX-0001-02), the Institut National du Cancer (INCa, subvention 2013-105), the Belgian Foundation against cancer (STK, FA/2014/294), the French National Research Agency (ANR-18-CE13-0017, Project SynTEV), the European Union's Horizon 2020 research and innovation program under the Marie Sklodowska-Curie grant agreement No 747025, the French Infrastructure for Integrated Structural Biology (FRISBI) ANR-10-INSB-05-01 with the use of the AFMB laboratory Xray facility. The authors acknowledge the European Synchrotron Radiation Facility (ESRF) as well as the SOLEIL

synchrotron (Proxima 1 and Proxima 2 beamlines) for provision of synchrotron radiation facilities. M. Garcia was the recipient of La Ligue, French Foundation for Cancer Research. R. Leblanc was the recipient of the Fondation ARC, French Foundation for Cancer Research.

References

[1] D.W. Greening, S.K. Gopal, R. Xu, R.J. Simpson, W. Chen, Exosomes and their roles in immune regulation and cancer, Semin Cell Dev Biol, 40 (2015) 72-81.
[2] I. Wortzel, S. Dror, C.M. Kenific, D. Lyden, Exosome-Mediated Metastasis: Communication from a Distance, Dev Cell, 49 (2019) 347-360.
[3] C. Rajagopal, K.B. Harikumar, The Origin and Functions of Exosomes in Cancer, Front Oncol, 8 (2018).
[4] J.J. Grootjans, P. Zimmermann, G. Reekmans, A. Smets, G. Degeest, J. Durr, G. David, Syntenin, a PDZ protein that binds syndecan cytoplasmic domains, Proc Natl Acad Sci U S A, 94 (1997) 13683-13688.
[5] K. Lambaerts, S. Van Dyck, E. Mortier, Y. Ivarsson, G. Degeest, A. Luyten, E. Vermeiren, B. Peers, G. David, P. Zimmermann, Syntenin, a syndecan adaptor and an Arf6 phosphatidylinositol 4,5-bisphosphate effector, is essential for epiboly and gastrulation cell movements in zebrafish, J Cell Sci, 125 (2012) 1129-1140.
[6] J.R. Couchman, Transmembrane signaling proteoglycans, Annu Rev Cell Dev Biol, 26 (2010) 89-114.
[7] H.C. Christianson, M. Belting, Heparan sulfate proteoglycan as a cell-surface endocytosis receptor, Matrix biology : journal of the International Society for Matrix Biology, 35 (2014) 51-55.
[8] V. Friand, G. David, P. Zimmermann, Syntenin and syndecan in the biogenesis of exosomes, Biol Cell, 107 (2015) 331-341.
[9] T.P. Kegelman, S.K. Das, L. Emdad, B. Hu, M.E. Menezes, P. Bhoopathi, X.Y. Wang, M. Pellecchia, D. Sarkar, P.B. Fisher, Targeting tumor invasion: the roles of MDA-9/Syntenin, Expert Opin Ther Targets, 19 (2015) 97-112.
[10] S.K. Das, S. Maji, S.L. Wechman, P. Bhoopathi, A.K. Pradhan, S. Talukdar, D. Sarkar, J. Landry, C.Q. Guo, X.Y. Wang, W.K. Cavenee, L. Emdad, P.B. Fisher, MDA-9/Syntenin (SDCBP): Novel gene and therapeutic target for cancer metastasis, Pharmacol Res, 155 (2020).
[11] L.N. Makley, J.E. Gestwicki, Expanding the number of 'druggable' targets: non-enzymes and protein-protein interactions, Chem Biol Drug Des, 81 (2013) 22-32.
[12] T. Cierpicki, J. Grembecka, Targeting protein-protein interactions in hematologic malignancies: still a challenge or a great opportunity for future therapies?, Immunol Rev, 263 (2015) 279-301.
[13] N. Bosc, C. Muller, L. Hoffer, D. Lagorce, S. Bourg, C. Derviaux, M.E. Gourdel, J.C. Rain, T.W. Miller, B.O. Villoutreix, M.A. Miteva, P. Bonnet, X. Morelli, O. Sperandio, P. Roche, Fr-PPIChem: An Academic Compound Library Dedicated to Protein-Protein Interactions, ACS Chem Biol, 15 (2020) 1566-1574.
[14] P. Filippakopoulos, J. Qi, S. Picaud, Y. Shen, W.B. Smith, O. Fedorov, E.M. Morse, T. Keates, T.T. Hickman, I. Felletar, M. Philpott, S. Munro, M.R. McKeown, Y. Wang, A.L. Christie, N. West, M.J. Cameron, B. Schwartz, T.D. Heightman, N. La Thangue, C.A. French, O. Wiest, A.L. Kung, S. Knapp, J.E. Bradner, Selective inhibition of BET bromodomains, Nature, 468 (2010) 1067-1073.

[15] O. Ulucan, S. Eyrisch, V. Helms, Druggability of dynamic protein-protein interfaces, Curr Pharm Des, 18 (2012) 4599-4606.
[16] M. Jung, K.A. Gelato, A. Fernandez-Montalvan, S. Siegel, B. Haendler, Targeting BET bromodomains for cancer treatment, Epigenomics, 7 (2015) 487-501.
[17] S. Milhas, B. Raux, S. Betzi, C. Derviaux, P. Roche, A. Restouin, M.J. Basse, E. Rebuffet, A. Lugari, M. Badol, R. Kashyap, J.C. Lissitzky, C. Eydoux, V. Hamon, M.E. Gourdel, S. Combes, P. Zimmermann, M. Aurrand-Lions, T. Roux, C. Rogers, S. Muller, S. Knapp, E. Trinquet, Y. Collette, J.C. Guillemot, X. Morelli, Protein-Protein Interaction Inhibition (2P2I)-Oriented Chemical Library Accelerates Hit Discovery, ACS Chem Biol, 11 (2016) 2140-2148.
[18] E.J. Faivre, K.F. McDaniel, D.H. Albert, S.R. Mantena, J.P. Plotnik, D. Wilcox, L. Zhang, M.H. Bui, G.S. Sheppard, L. Wang, V. Sehgal, X. Lin, X. Huang, X. Lu, T. Uziel, P. Hessler, L.T. Lam, R.J. Bellin, G. Mehta, S. Fidanze, J.K. Pratt, D. Liu, L.A. Hasvold, C. Sun, S.C. Panchal, J.J. Nicolette, S.L. Fossey, C.H. Park, K. Longenecker, L. Bigelow, M. Torrent, S.H. Rosenberg, W.M. Kati, Y. Shen, Selective inhibition of the BD2 bromodomain of BET proteins in prostate cancer, Nature, 578 (2020) 306-310.
[19] R. Leblanc, R. Kashyap, K. Barral, A.L. Egea-Jimenez, D. Kovalskyy, M. Feracci, M. Garcia, C. Derviaux, S. Betzi, R. Ghossoub, M. Platonov, P. Roche, X. Morelli, L. Hoffer, P. Zimmermann, Pharmacological inhibition of syntenin PDZ2 domain impairs breast cancer cell activities and exosome loadifing with syndecan and EpCAM cargo, J Extracell Vesicles, 10 (2020) e12039.
[20] X.S. Chen, J.C. Longgood, C. Michnoff, S.G. Wei, D.E. Frantz, I. Bezprozvanny, High-throughput screen for small molecule inhibitors of Mint1-PDZ domains, Assay Drug Dev Techn, 5 (2007) 769-783.
[21] J.P. Borg, PDZ Mediated Interactions, Springer Protocols, 2256 (2021).
[22] E.Y.S. Lin, L.F. Silvian, D.J. Marcotte, C.C. Banos, F. Jow, T.R. Chan, R.M. Arduini, F. Qian, D.P. Baker, C. Bergeron, C.A. Hession, R.L. Huganir, C.F. Borenstein, I. Enyedy, J. Zou, E. Rohde, M. Wittmann, G. Kumaravel, K.J. Rhodes, R.H. Scannevin, A. Dunah, K.M. Guckian, Potent PDZ-Domain PICK1 Inhibitors that Modulate Amyloid Beta-Mediated Synaptic Dysfunction, Sci Rep-Uk, 8 (2018).
[23] T.P. Kegelman, B. Wu, S.K. Das, S. Talukdar, J.M. Beckta, B. Hu, L. Emdad, K. Valerie, D. Sarkar, F.B. Furnari, W.K. Cavenee, J. Wei, A. Purves, S.K. De, M. Pellecchia, P.B. Fisher, Inhibition of radiation-induced glioblastoma invasion by genetic and pharmacological targeting of MDA-9/Syntenin, Proc Natl Acad Sci U S A, 114 (2017) 370-375.
[24] I. Elidrisi, P.V. Bhatt, T. Govender, H.G. Kruger, G.E.M. Maguire, Synthesis and NMR elucidation of novel amino acid cavitand derivatives, Tetrahedron, 70 (2014) 7057-7066.
[25] I. Elidrisi, S. Negin, P.V. Bhatt, T. Govender, H.G. Kruger, G.W. Gokel, G.E.M. Maguire, Pore formation in phospholipid bilayers by amphiphilic cavitands, Org Biomol Chem, 9 (2011) 4498-4506.
[26] C. Lamberth, H.J. Kempf, M. Kriz, Synthesis and fungicidal activity of N-2-(3-methoxy-4-propargyloxy) phenethyl amides. Part 3: stretched and heterocyclic mandelamide oomyceticides, Pest Manag Sci, 63 (2007) 57-62.
[27] Y.L. Song, Y.F. Dong, T. Yang, C.C. Zhang, L.M. Su, X. Huang, D.N. Zhang, G.L. Yang, Y.X. Liu, Synthesis and pharmacological evaluation of novel bisindolylalkanes analogues, Bioorgan Med Chem, 21 (2013) 7624-7627.
[28] K. Matsumoto, S. Suga, J. Yoshida, Organic reactions mediated by electrochemically generated ArS+, Org Biomol Chem, 9 (2011) 2586-2596.
[29] Y.X. Liu, Z.P. Cui, Y.H. Li, Y.C. Gu, Q.M. Wang, 3-Hydrazido and 3-Hydrazono Derivatives of Tenuazonic Acid and their Herbicide Evaluation, J Heterocyclic Chem, 51 (2014) E197-E201.

[30] L. Hoffer, Y.V. Voitovich, B. Raux, K. Carrasco, C. Muller, A.Y. Fedorov, C. Derviaux, A. Amouric, S. Betzi, D. Horvath, A. Varnek, Y. Collette, S. Combes, P. Roche, X. Morelli, Integrated Strategy for Lead Optimization Based on Fragment Growing: The Diversity-Oriented-Target-Focused-Synthesis Approach, J Med Chem, 61 (2018) 5719-5732.
[31] L. Hoffer, J.P. Renaud, D. Horvath, In Silico Fragment-Based Drug Discovery: Setup and Validation of a Fragment-to-Lead Computational Protocol Using S4MPLE, J Chem Inf Model, 53 (2013) 836-851.
[32] L. Hoffer, C. Chira, G. Marcou, A. Varnek, D. Horvath, S4MPLE-Sampler for Multiple Protein-Ligand Entities: Methodology and Rigid-Site Docking Benchmarking, Molecules, 20 (2015) 8997-9028.
[33] A.L. Egea-Jimenez, R. Gallardo, A. Garcia-Pino, Y. Ivarsson, A.M. Wawrzyniak, R. Kashyap, R. Loris, J. Schymkowitz, F. Rousseau, P. Zimmermann, Frizzled 7 and PIP2 binding by syntenin PDZ2 domain supports Frizzled 7 trafficking and signalling, Nat Commun, 7 (2016) 12101.
[34] D. Kozakov, L.E. Grove, D.R. Hall, T. Bohnuud, S.E. Mottarella, L. Luo, B. Xia, D. Beglov, S. Vajda, The FTMap family of web servers for determining and characterizing ligand-binding hot spots of proteins, Nat Protoc, 10 (2015) 733-755.
[35] M. Matziari, F. Beau, P. Cuniasse, V. Dive, A. Yiotakis, Evaluation of P-1'-diversified phosphinic peptides leads to the development of highly selective inhibitors of MMP-11, J Med Chem, 47 (2004) 325-336.
[36] M. Hartenfeller, M. Eberle, P. Meier, C. Nieto-Oberhuber, K.H. Altmann, G. Schneider, E. Jacoby, S. Renner, A Collection of Robust Organic Synthesis Reactions for In Silico Molecule Design, J Chem Inf Model, 51 (2011) 3093-3098.
[37] N.S. Imjeti, K. Menck, A.L. Egea-Jimenez, C. Lecointre, F. Lembo, H. Bouguenina, A. Badache, R. Ghossoub, G. David, S. Roche, P. Zimmermann, Syntenin mediates SRC function in exosomal cell-to-cell communication, Proc Natl Acad Sci U S A, 114 (2017) 12495-12500.

List of captions for Figures, Schemes and Tables

Figure 1. A. Crystal structure of syntenin PDZ2 domain in complex with compound **C58** (PDBID: 6R9H). Compound **C58** is depicted in cylinder representation dark green carbon atom. Nitrogen, oxygen, chlorine and sulfur are colored in blue, red, green and yellow, respectively. Small red spheres represent water molecules around the binding sites. Hydrogen bond interactions are displayed as black dotted lines. Amino acid residues highlighted are those establishing Van der Waals interactions with compound **C58**. **B**. 2D structure of hit fragment **C58**. **C**. 2D structures of putatively interesting explored modifications around fragment **C58**.

Figure 2. Selectivity profiles and IC_{50} of compounds **C58** (red) and **45** (blue) using HTRF assay without and with 0.01% NP40.

Figure 3. Crystal structure of syntenin PDZ2 domain in complex with compound **45** (PDBID: 6RLC). Compound **45** is displayed in cylinder representation orange carbon atom. Nitrogen, oxygen, chlorine and sulfur are colored in blue, red, green and yellow, respectively. Small red spheres represent water molecules around the binding sites. Hydrogen bond interactions are depicted as black dotted lines. Amino acid residues indicated are those establishing Van der Waals interactions with compound **45**.

Figure 4. A. General scheme for synthesis of derivatives **57** and **58-66** *via* Suzuki-Miyaura coupling. **B**. Structure, IC_{50} and LE values of analogues **57-66** on Syntenin-Syndecan2 complex HTRF assay. (a) in parenthesis IC_{50} and LE values with NP40 0.01%. Additional physicochemical efficiency metrics are shown Table S1 in Supp. Data.

Figure 5. MCF-7 cells were treated with vehicle (Ctrl) or the indicated compound (**32**, **45**, **56** & **57**; 100µM) in medium containing exosome-depleted FCS (10%) for 16h. **A**. Exosomes and corresponding total cell lysates were analyzed by western blot, tracing different markers, as indicated. **B.** Histograms represent mean signal intensities (±SEM) in exosomes, relative to controls (Ctrl). Data were obtained from N independent experiments, as indicated. Statistical analysis was performed using the one-way analysis of variance (ANOVA) with a Tukey posttest.

Scheme 1. Synthesis of analogues **13-20**.

Scheme 2. Synthesis of analogues **41-53** and their ester derivatives **28-40**.

Table 1. Inhibition of Syntenin-Syndecan2 complex interaction in the presence of analogues **13-20** and **41-53** at 400 µM confirmed in counter screening experiment using HTRF assay.

Table 2. 2D structure of selected compounds by the virtual growing strategy. Building blocks used to build the compounds are depicted with reactive groups (boronic acid or ester) leading to aromatic-carbon bonds highlighted in red.